Characterisation of lesions and associated immune cell populations in the lung of African buffalo (*Syncerus caffer*) infected with *Mycobacterium bovis*

by

Samantha Goldswain

Thesis presented in fulfilment of the requirements for the degree of Master of Science (Molecular Biology) in the Faculty of Medicine and Health Sciences at Stellenbosch University

Supervisor: Prof Michele Ann Miller

Co-supervisors: Dr. Léanie Kleynhans and Dr. Jennifer Landolfi

March 2021

Declaration

By submitting this thesis electronically, I declare that the entirety of the work contained therein is my own, original work, that I am the sole author thereof (save to the extent explicitly otherwise stated), that reproduction and publication thereof by Stellenbosch University will not infringe any third-party rights and that I have not previously in its entirety or in part submitted it for obtaining any qualification.

March 2021

Abstract

A vast array of species is susceptible to *Mycobacterium bovis* (*M. bovis*) infection, with varying pathogenesis and disease outcomes. Understanding the pathogenesis of disease is important for informing epidemiologic concerns and disease management strategies, especially in reservoir hosts, such as African buffaloes (*Syncerus caffer*). Therefore, this project is focused on characterisation of histologic morphology and associated immune cell populations in lung granulomas from *M. bovis* infected African buffalo to advance knowledge of disease development in buffaloes. A scoring system was developed to compare numbers and distributions of different immune cells, as well as other pathologic changes in bovine tuberculosis (bTB) pulmonary granulomas. In addition, an immunohistochemistry (IHC) staining technique was optimised for immune cell surface marker detection in buffalo lung tissues.

Formalin-fixed and frozen tissues were available from *M. bovis* naturally infected buffaloes from Hluhluwe-iMfolozi Park, South Africa. Formalin-fixed lung tissues were selected based on gross lesion scores that represented a range of severity. Lung sections from 14 buffaloes were stained with haematoxylin and eosin (H&E) to assess the histologic morphology of granulomas. Microscopic characteristics were then scored based on six categories. In addition, immunohistochemical techniques were optimised using antibodies that detected immune cell surface antigens (CD3, CD4, CD21, CD163, NCR1).

This study documented characteristics of a low histologic stage granuloma to include macrophages/multinucleated giant cells (MNGCs) at the core, lymphocytic infiltration surrounding the macrophages, and minimal to no necrosis and fibrosis. Granulomas compatible with more advanced disease were necrotic, with macrophages surrounding the necrotic core, lymphocytes located peripherally, and were encapsulated by a fibrous capsule. More developed granulomas were not always mineralised. Based on IHC, CD3+ T lymphocytes and CD163+ macrophages/MNGCs were present in all granulomas examined; B cells (CD21+) were only present in higher stage granulomas; and natural killer (NCR1+) cells were not abundant in any of granulomas. The CD4 antibody did not stain buffalo tissues and therefore, distribution of this subset of T lymphocytes could not be evaluated. Ziehl-Neelsen staining was performed to detect the presence of acid-fast bacilli, however, no bacilli were visible in the slides analysed. The appearance of the buffalo pulmonary granulomas did not completely fit with the stages

described in cattle (Wangoo *et al.,* 2005). Therefore, a scoring system for categorising granulomas, adapted for buffaloes, should be investigated to provide a species-specific description that would be beneficial for understanding bTB pathogenesis.

In summary, findings showed that lymphocytes and macrophages/MNGCs appear to be the predominant immune cell types present and their distribution and relative numbers appear to change as pulmonary granulomas develop. Characteristics such as increased fibrous encapsulation and development of a necrotic core appear to be similar to granulomas in cattle. However, mineralisation may not be a consistent feature, suggesting some species-specific differences that should be further investigated. This study also demonstrated that immunohistochemistry is a practical method for further characterisation of local immune responses to *M. bovis* infection in buffalo. Further research with a larger sample set will be informative for understanding local and associating systemic immune responses to bTB in buffaloes.

Opsomming

Baie spesies is vatbaar vir Mikobakterium bovis (*M. bovis*) infeksie, en die progressie en die uitkomste van die siekte kan grootliks verskil. Dit is belangrik om die verloop van die siekte te verstaan, om epidemiologiese bekommernisse aan te spreek en strategieë om die siekte te bestuur te bepaal, veral in gasheerspesies soos Afrika-buffels (*Syncerus caffer*). Hierdie projek fokus dus daarop om die histologiese morfologie en gepaardgaande immuunselpopulasies in longgranulome van *M. bovis*-geïnfekteerde Afrika-buffels te karakteriseer om die vordering van die siekte te verstaan. 'n Puntestelsel om die aantal en verspreiding van verskillende immuunselle en ander patologiese veranderinge in pulmonêre granulome in beestuberkulose (bTB) te vergelyk is ontwikkel. Daarbenewens is 'n immunohistochemie (IHC) kleuringstegniek geoptimiseer om immuun seloppervlakmerkers in gevriesde en formalien-gestoorde longweefsels van buffels te identifiseer.

Formalien-gestoorde en gevriesde long weefsels van buffels van Hluhluwe-iMfolozi Park, Suid-Afrika, wat natuurlik met *M. bovis* geïnfekteer is, is gebruik. Formalien-gestoorde longweefsels is geselekteer op grond van hul makroskopiese letselpunte wat verskillende vlakke van erns verteenwoordig. Longseksies van 14 buffels is met haemotoxylin en eosin (H&E) gekleur om die morfologie van granulome te bepaal. Mikroskopiese eienskappe is gebaseer op sewe kategorieë. ‘n Immunohistochemiese tegniek wat gebruik maak van teenliggaampies wat immuun-seloppervlak-antigene (CD3, CD4, CD21, CD163, NCR1) identifiseer is ook geoptimaliseer.

Hierdie studie wys dat vroeë granulome makrofage/multi-kerne reus-selle (MNGCs) in hul kerns het, dat limfositiese infiltrasie rondom die makrofage voorkom met minimale tot geen nekrose en fibrose. Granulome versoenbaar met gevorderde siekte is nekroties met makrofage/MNGCs rondom die nekrotiese kern. Limfosiete is perifere geleë, en granulome is deur fibrose omsluit. Gevorderde letsels is nie altyd gemineraliseer nie. CD3+ T-limfosiete en CD163+ macrophage/MNGCs was teenwoordig in alle granulome; B-selle (CD21+) is slegs teenwoordig in gevorderde granulome. Natuurlike moordenaarselle (NCR1+) was min in alle granulome. Fibrose het toegeneem namate die ontwikkeling van granulome gevorder het. Die CD4-teenliggaampies het nie gwerk nie en kon die verspreiding van die T-selpopulasie nie geëvalueer word nie. Ziehl-Neelson-kleuring is gedoen om die teenwoordigheid van suurvaste bakterië op te spoor, maar geen was sigbaar in die skyfies wat ondersoek was nie. Die

beskrywing van pulmonale buffel granulome het nie ooreegestem met die stadiums van ontwikkeling wat vir beeste beskryf is nie (Wagoo et al., 2005). 'n Aangepaste puntestelsel vir die kategorisering van granulome in buffels moet dus ondersoek word om 'n spesiespesifieke beskrywing te kry. Dit sal help om die progressie van bTB in buffels te verstaan.

Ter opsomming, hierdie study toon dat limfosiete en makrofage/MNGCs die oorheersende immuunseltipes is en dat hul verspreiding en relatiewe getalle verander in vroeë en gevorderde pulmonale granulome van *M-bovis*-geïnfekteerde buffels. Eienskappe soos die toename in fibrose en die ontwikkeling van nekrotiese kerns stem ooreen met die beskrywing van granulome in beeste. Mineralisering is egter nie 'n algemene kenmerk tussen buffels en beeste nie, en dui op spesiespesifieke verskille wat ondersoek moet word. Hierdie studie toon ook dat immunohistochemie 'n praktiese metode is vir karakterisering van die plaaslike immuunresponse teen *M. bovis*-infeksie in buffels. Verdere navorsing met 'n groter steekproef sal insiggewend wees om die plaaslike responses en die assosiasie met sistemiese immuunresponse gedurende bTB in buffel te verstaan.

Table of Contents

Acknowledgements

I would like to thank my supervisors for your guidance, encouragement, and support over the duration of my MSc study. Your guidance has enabled me to grow professionally and personally, and you have taught me to take responsibility. I would also like to thank the entire Animal TB Research Group for playing a role in my professional development.

Thank you to everyone involved in my sample collection at Hluhluwe-iMfolozi Park, namely Dr. Dave Cooper, Alicia and Warren McCall, Dr. Rowan Leeming, Dr. Sarah Wilkinson, the Ezemvelo KZN Wildlife game capture team, Dr. Wynand Goosen, and Katrin Smith.

I would like to thank Reggie Williams and Jeffrey Pieterse from the Division of Clinical Anatomy and for all your help in assisting with my lab work.

Thank you to Jurgen Geitner, from UCT for assisting with the scanning of my slides for their subsequent analysis.

My gratitude goes out to my family for providing me the opportunity to further my education and for the constant support, advice and love you have given me.

Finally, I would like to thank all my friends for all the encouragement you have given me throughout the past two years.

List of Abbreviations

%	percentage
℃	degrees Celsius
μg	microgram
μg/ml	microgram per milliliter
μl	microliter
μM	micromolar
ACTB	beta actin
AM	alveolar macrophages
APC	antigen-presenting cell
bTB	bovine tuberculosis
CMI	cell-mediated immunity
CCL2	C-C motif ligand 2
CCL10	C-C motif ligand 10
cm	centimeter
CXCL	C-X-C motif ligand 10
DAB	diaminobenzidine tetrahydrochloride
DPX	dibutylphatalate polystyrene xylene
EDTA	ethylenediaminetetraacetic acid
ELISA	enzyme-linked immunosorbent assay
ER	epitope retrieval
H&E	haematoxylin and eosin
HiP	Hluhluwe-iMfolozi Park
HRP	horseradish peroxidase
IFN-γ	interferon gamma
IgG	immunoglobin G
IgM	immunoglobin M
IGRA	interferon gamma release assay
IHC	immunohistochemistry
IL	interleukin
IPRA	interferon gamma-induced protein 10kDa release assay
KNP	Kruger National Park
LN	lymph node
M. bovis	*Mycobacterium bovis*
mg	milligrams
MHC	major histocompatibility complex

min	minutes
ml	milliliter
mm	millimeter
mM	millimolar
MNGC	multinucleated giant cell
mRNA	messenger RNA
MTBC	*Mycobacterium tuberculosis* complex
M. tuberculosis	*Mycobacterium tuberculosis*
ng	nanogram
NK	natural killer
nm	nanometer
NRF	National Research Foundation
PCR	polymerase chain reaction
pg	picogram
PPD	purified protein derivative
QFT	QuantiFERON®-TB Gold
RT	room temperature
SAMRC	South African Medical Research Council
SANParks	South African National Parks
SICTT	single intradermal comparative tuberculin test
SD	standard deviation
TB	tuberculosis
TGF-β	transforming growth factor-beta
Th	T-helper
TNF-α	tumor necrosis factor alpha
TNF-β	tumor necrosis factor beta
TST	tuberculin skin test
WHO	World Health Organisation
WSU	Washington State University
ZEN™	ZEISS Efficient Navigation
ZN	Ziehl-Neelsen

List of Figures

List of Tables

Chapter 1: Introduction

General background

Control of bovine tuberculosis (bTB) has drastically reduced its prevalence in livestock and humans, particularly in industrialised countries; however, in developing countries, especially in southern Africa, bTB still remains a challenge to animal health (Musoke *et al.,* 2015). *Mycobacterium bovis* (*M. bovis*), the causative agent of bTB, is a member of the *Mycobacterium tuberculosis* complex (MTBC), a group of *Mycobacterium* species that cause tuberculosis (TB) in a range of mammals (Brites and Gagneux, 2017). African buffaloes (*Syncerus caffer*) are recognised wildlife maintenance hosts for *M. bovis* in South Africa and the infection is primarily spread between buffaloes via the respiratory route (Michel *et al.,* 2007; Tadayon *et al.,* 2006).

Hluhluwe-iMfolozi Park (HiP) and Kruger National Park (KNP) are South Africa's two largest game reserves, both endemic areas for *M. bovis* (Michel *et al.,* 2006). HiP has a bTB prevalence in buffaloes ranging from 2.3% to 54.7%, depending on the geographic location (le Roex *et al.,* 2016). KNP has a bTB prevalence in buffalo ranging from 1.5% in the north of Kruger to 38.2% in the south (Rodwell *et al.,* 2001). The reserves are adjacent to community lands where livestock graze freely and are only separated from wildlife by fences, which are often damaged (Jori *et al.,* 2011). Studies have provided evidence that infected wildlife in KNP are a risk factor for *M. bovis* infection of neighboring cattle (Musoke *et al.,* 2015). It is also believed that infection of predators occurs orally by the consumption of infected buffaloes (Michel *et al.,* 2006). Bovine TB can be spread indirectly to humans by ingestion of unpasteurised milk from cattle or undercooked meat, or exposure to respiratory secretions during handling of an infected animal (Khatri *et al.,* 2018).

The characteristic lesion resulting from mycobacterial infection and associated host responses is granulomatous inflammation, including organised granulomas. Such inflammation is not unique to mycobacterial infection as similar host responses may also be elicited by other pathogens or foreign material (Palmer *et al.* 2016). Granulomas are comprised of varied cell types including but not limited to epithelial macrophages, multinucleated giant cells, and lymphocytes (Palmer *et al.* 2016). In cattle, bTB granulomas have been classified into four categories according to lesion morphology (Wangoo *et al.,* 2005). These stages are (1) the initial stage, (2) the solid stage, (3) the minimal necrosis stage and (4) the necrosis and

mineralisation stage (Wangoo *et al.,* 2005). However, lesions associated with bTB have not been well described in African buffaloes. Additionally, stages of infection and disease progression are unknown and merit further study. Since African buffaloes are the key wildlife maintenance hosts of *M. bovis* in South Africa, they are an important species to focus on for disease management. Control of infection in reservoir species, such as African buffaloes, may limit disease and consequences in other wildlife species, livestock, and humans.

Using conventional histologic techniques, such as staining with haematoxylin and eosin (H&E), immune cell types can be generally identified based on morphology, but immunohistochemical techniques provide more specific characterisation using specific cell surface markers. To study granuloma structure and correlate with stage of disease, immunohistochemical techniques have been used in cattle to describe stages of pulmonary bTB (Wangoo *et al*., 2005). Similar techniques can also be applied to tissue samples from *M. bovis*-infected buffaloes to facilitate characterisation of the granulomas and investigate comparative host responses in different, though related species. Staining with a range of antibodies to specific immune cell surface antigens will allow the detection of different cell types and evaluation of their distribution in granulomas in *M. bovis*-infected African buffaloes (Duraiyan *et. al.* 2012).

Immunohistochemistry background

Immunohistochemistry (IHC) is a technique used to detect the presence of specific immune cell markers. Target antigens are proteins that are within or on the surface of a cell and the first stage of IHC is the application of a primary antibody that binds specifically to the target antigen. Antibodies may be used to stain tissues from different species, depending on the conservation of the epitope. Therefore, adequate research should be done when selecting antibodies (Kim *et al.,* 2016). Antibodies can either be mono- or polyclonal. Polyclonal antibodies can bind to multiple epitopes on the target antigen and are therefore more likely to also cross-react to non-target antigens (Kabiraj *et al.,* 2015). Monoclonal antibodies are produced to bind to a single epitope and tend to have more specific staining but can be less sensitive, especially if used in a different species to which the antibody was developed (Kabiraj *et al.,* 2015). Secondary antibodies are often used which are conjugated to a substance to allow signal detection (Kim *et al.,* 2016).

The detection system in IHC is based on the binding of the secondary antibody to the specific primary antibody and utilises enzymes such as horseradish peroxidase (HRP) conjugated to the secondary antibody (Kim *et al.,* 2016). Multiple enzymes can be attached to the antibody and may produce more intense staining since there are more molecules for the chromogen to attach to (Kabiraj *et al.,* 2016). The chromogen is the substrate that forms an insoluble coloured precipitate that can be visualized under a microscope, for example 3,3'-diaminobenzidine tetrahydrochloride (DAB), which results in brown staining (Kabiraj *et al.,* 2015).

Controls should be included with each IHC staining procedure. A negative control ensures that staining observed is not due to background or nonspecific staining. A positive control verifies the binding of the antibodies and activity of the secondary reagents (Hewitt *et al.*, 2014).

The fixation of tissues is required to stop the diffusion of soluble components, block unwanted enzyme activity, stop the degradation of tissue structures, and allow preparation to withstand the steps of the staining procedure (Kabiraj *et al.*, 2016). Formalin-fixed tissue retains morphological characteristics but antigens experience denaturation and this may diminish epitope recognition by the primary antibody (Werner *et al.,* 2000). This can be solved by either of two approaches; by using antibodies raised specifically to recognise formalin-fixed antigens or using a protocol designed to expose antigens in fixed tissues, such as the antigen retrieval method (Hofman, 2002).

Formalin forms intra-molecular crosslinks with amino groups of proteins and hinder the accessibility of the antigen for the antibody (Kabiraj *et al.,* 2015). The longer the fixation, the more cross-linking takes place. Heat treatment is a common method used for antigen retrieval in IHC studies of formalin-fixed tissues and works by breaking the crosslinks of the proteins (Hofman, 2002). Temperature, pH, and buffer composition contribute to successful antigen retrieval. Antigen retrieval, however, may influence the tissue morphology and increase background staining (Kabiraj *et al.,* 2015).

Problem statement

There are significant knowledge gaps pertaining to differences in TB pathogenesis among affected species. Pathological changes can provide needed insight and begin to bridge such knowledge gaps. Understanding comparative pathogenesis and immunology of TB in different species is essential to diagnosing infection and disease, as well as informing disease management strategies. In the case of bTB in buffalo, it is unclear if the disease follows the

same patterns as cattle, how host-pathogen interactions lead to certain disease outcomes, and whether infection and disease outcomes differ by strain of the pathogen. Therefore, it is imperative to investigate and understand the host's immune response at a tissue level. Host contributions to lesion formation influence morphology and can correlate with different stages of disease. Defining and understanding lesion morphology can provide insight into disease progression, identify potential diagnostic biomarkers for different stages of disease, and provide a foundation for comparative immunopathology among susceptible species (e.g. buffalo and cattle). This leads to our research question which is how the morphologic and immunohistochemical characterisation of pulmonary granulomas from *M. bovis*-infected buffaloes (*Syncerus caffer*) differ and inform localised stages of disease?

Study Aims and Objectives

Aim 1:

To characterise bTB granulomas in lung tissue by determining the presence, relative numbers, and distribution of specific immune cell types in granulomas from naturally *M. bovis*-infected buffaloes.

Objective 1.1:

To examine lesions from buffalo grossly diagnosed as bTB and confirm or refute the preliminary diagnosis histologically.

Objective 1.2:

To provide a morphologic description of lesions associated with bTB in buffalo via routine light microscopy.

Objective 1.3:

To score histologic lesions based upon microscopic features described in cattle bTB granulomas.

Objective 1.4:

To compare histologic lesion scores to gross lesion scores in cases of confirmed bTB.

Aim 2:

To establish an immunohistochemistry staining technique for immune cell surface markers specific for buffalo lung tissues.

Objective 2.1:

To optimise an immunohistochemistry technique protocol for use with buffalo lung tissues.

Chapter 2: Literature Review

Introduction

Mycobacterium bovis (*M. bovis*) is the causative agent for bovine tuberculosis (bTB) in wild and domestic animals (Cartensen and DonCarlos, 2011). However, there is a lack of comprehensive knowledge regarding disease development and infection outcomes in many animal species, especially wildlife. Since the dynamics of *Mycobacterium tuberculosis* (*M. tb*) infection in humans has been extensively studied, it may serve as a model for *M. bovis* infection in animals (Waters and Palmer, 2015). There are various outcomes of *M. tb* infection in humans with primary clearance being 90% of cases (Michelsen *et al.,* 2017). In some cases, the immune system can efficiently remove the bacteria, and the infection will be cleared (Sasindran and Torrelles, 2019). Others, however, will become latently infected (Michelsen *et al.,* 2017). In these cases, bacteria are present in tissues but are not replicating (Sasindran and Torrelles, 2019). Two additional clinical states have been reported in humans; namely, incipient and subclinical disease (Drain *et al.,* 2018). Incipient tuberculosis (TB) results with the patient having viable or replicating bacteria that is likely to progress to active disease but does not display any microbiological or radiological evidence of disease (Drain *et al.,* 2018). In contrast, a subclinical state of disease is characterised by infection that can be detected using radiologic or microbiologic techniques but occurs in the absence of any signs or symptoms of illness (Drain *et al.,* 2018). Our understanding of incipient and subclinical TB is limited, and current diagnostic tests do not distinguish these states. A wide range of tests, including national surveys, active case-finding studies, and systematic screening of high-risk groups have been used to gain insight into the epidemiology of incipient and subclinical TB (Drain *et al.,*2018). Finally, in individuals with active disease, infection is associated with clinical signs such as coughing, fever, weight loss, chest pain, and night sweats as disease progresses (Heemskerk *et al.,* 2019). According to the World Health Organization (WHO), active TB is defined by the detection of viable bacteria causing clinical symptoms with radiographic abnormalities or microbiologic evidence of infection, and the patient, more often than not, is infectious (WHO, 2010). However, only 5% of infected people progress to active disease (Drain *et al.,* 2018). The various stages of infection and disease in human TB are dynamic and determined by the interaction of the host immune response and physiological state of the mycobacteria. Through an understanding of disease progression in humans, some insight may be gained regarding the pathogenesis of bTB in animals, since TB and bTB share similar aspects such as immune responses and lesion development (Waters and Palmer, 2015). In humans, pulmonary TB is

statistically more common than extra-pulmonary TB and disseminated TB (Rajasekaran *et al.,* 2007). However, analogous clinical manifestations of disease as described in human TB may not always occur in animal TB, complicating determination of disease stage and progression. Active disease is presumed in animals with clinically evident illness and microbiological confirmation of infection (Alvarez *et al.,* 2009). However, appropriate tools to provide confirmation of the existence of latent infection and incipient disease in animals are currently lacking (Alvarez *et al.,* 2009).

With domestic cattle as the primary reservoir host, *M. bovis* can be transmitted to multiple species, including other domestic animals and wildlife (Palmer *et al.,* 2016). In South Africa, susceptible wildlife species include African buffalo (*Syncerus caffer*), lion (*Panthera leo*) and the greater kudu (*Tragelaphus strepsiceros*) (Musoke *et al.,* 2015). Importantly, infection is often subclinical in these wildlife hosts allowing for infected, apparently healthy animals to serve as a source of infection for other animals or possibly humans (de Vos *et al.,* 2001; Ayele *et al.,* 2004). The usual route of infection is via the inhalation of bacteria in droplets that are expelled from the lungs of an infected animal (Menzies and Neill, 2000). Bovine TB can also be spread indirectly by ingestion of milk or meat from an infected animal (Khatri *et al.,* 2018). Infection primarily occurs in the lung but can affect multiple organs depending on the route of infection (Ganchua *et al.,* 2018). Both wild and domestic animals with active bTB may have reduced milk production and fecundity, loss of body condition, coughing or other respiratory signs, which may progress to death (Michel *et al.,* 2009). The disease in livestock negatively impacts the economy, particularly in developed countries, through restrictions on trade and animal movement together with reduced production and increased biosecurity costs (de Vos *et al., 2001*; Ayele *et al.,* 2004).

Granulomatous pneumonia is a specific type of pneumonia caused by organisms that cannot normally be eliminated by phagocytosis (Lopez and Martinson, 2017). The host responds to the organism by evoking an inflammatory reaction in which the host pulmonary defenses are facilitated by resident alveolar macrophages (AMs). AMs act to limit and localise infection as additional mononuclear and polymorphonuclear phagocytes are recruited to the site of infection (Cooper, 2009). The term granulomatous describes a pattern of pneumonia that is characterised by the presence of masses or nodules of chronically inflamed tissue with granulations that are associated with an infectious process. Granulomatous pneumonia is characterised by the presence of variable numbers of caseous and noncaseous granulomas

distributed throughout the lungs (Lopez and Martinson, 2017). Granulomatous pneumonia is seen in some bacterial diseases and the hallmark lesion of mycobacterial infection is a granuloma (Ramakrishnan, 2012). However, granulomas can arise in response to many infectious agents and noninfectious stimuli including other bacteria, fungi, protozoa, parasites, and foreign material (Pagán and Ramakrishnan, 2008). Granuloma formation is a complex process orchestrated by multiple immune cell types including, but not limited to, macrophages, neutrophils, natural killer (NK) cells, and lymphocytes, and is utilised by the body to isolate and clear intracellular pathogens, such as *M. bovis* (Palmer *et al.,* 2006; Wangoo *et al.,* 2005).

If an animal has an overwhelming bacterial load, excessive inflammation due to an influx of immune cells to the site of infection may cause host-mediated tissue damage that can contribute to disease progression (Carow *et al.,* 2019). Initially it was thought that the granuloma was a host-protective structure that confined the bacteria (Clay *et al.,* 2008). However, it is now believed that the granuloma may represent a dynamic balance between the immune response that attempts to contain or kill the invading pathogen and the pathogen establishing a niche where they can survive and potentially disseminate (Clay *et al.,* 2008).

Granuloma Formation

The minimal requirement for a structure to be classified as a granuloma is the accumulation of mature macrophages. A mature macrophage shows an increase in cytoplasmic volume, greater numbers of organelles and a ruffled cell membrane, morphological features of immune reactivity for enhanced phagocytosis and microbicidal activity (Pagán and Ramakrishnan, 2008). Pulmonary granuloma formation requires a complex cascade of events following the inhalation of a pathogen and involves many biological interactions between the host cells and the invading organism (Ramakrishnan, 2012).

Generally, a granuloma consists of organised aggregates of cells including macrophages and lymphocytes that attempt to eliminate foreign agents (Ramakrishnan, 2012) (Figure 2.1). Cellular components of granulomas may also include multinucleated giant cells (MNGCs), epithelioid cells, lymphocytes, fibroblasts and dendritic cells (DCs) (Figure 2.2) and may develop accessory features such as necrosis or mineralisation (Ramakrishnan, 2012).

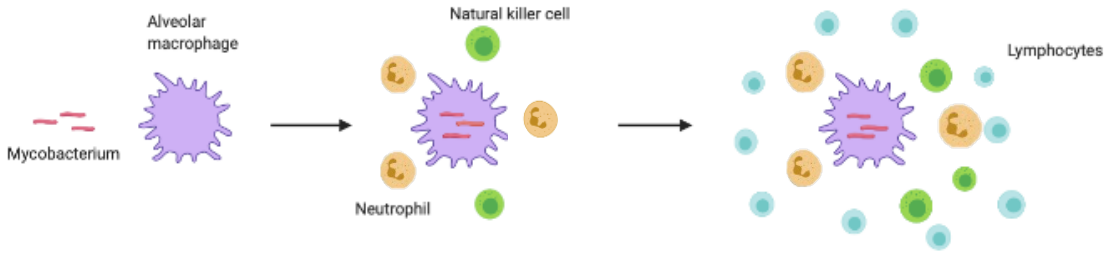

Figure 2.1. Diagram illustrating the initial stages of granuloma formation in an immunocompetent individual infected with *Mycobacterium* spp., starting from alveolar macrophage infection leading to the infiltration of lymphocytes at the site of infection. Original figure designed with software at BioRender.com.

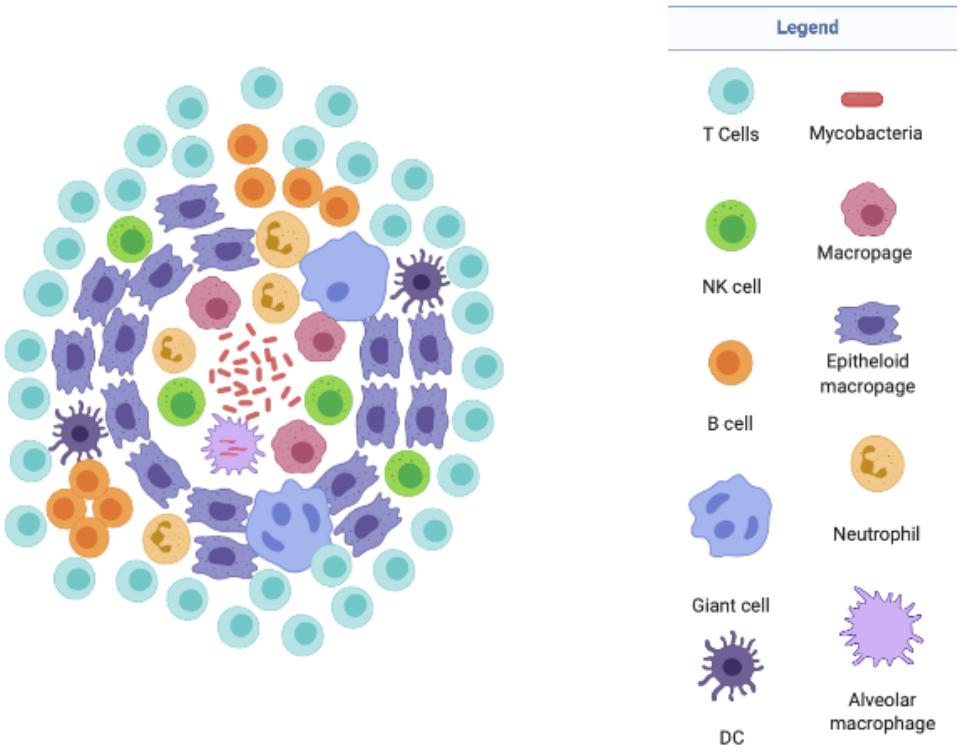

Figure 2.2. Image showing the typical immune cell types involved in mycobacterial granuloma formation, highlighting their general distribution and relative abundance. Original figure designed with software at BioRender.com.

The host's immune system consists of innate and adaptive immune components, with the innate system being the body's first line of defence against invading pathogens. The cell types involved in the innate immune response include macrophages, NK cells, neutrophils, eosinophils, and basophils (Janeway *et al.,* 2019). Innate immunity is antigen non-specific and functions to immediately prevent the spread of pathogens in the body (Janeway *et al.,* 2019). Alveolar macrophages are long-lived innate immune cells that can ingest inhaled bacteria and set the stage for the subsequent immune response (Mayer-Barber and Barber, 2015) (Figure 2.1). The induction of adaptive immunity starts when the pathogen is ingested by an immature DC in the infected tissue (Janeway *et al.,* 2019) (Figure 2.2). Dendritic cells migrate through the lymph to regional lymph nodes where they interact with naïve lymphocytes (Janeway *et al.,* 2019). Adaptive immunity is an antigen-specific, delayed response mediated by lymphocytes and has a role in protection against pathogens including bacteria (Janeway *et al.,* 2019). Although a few key pathways have been identified, there are still knowledge gaps about the mechanisms of T-cell-dependent control of mycobacterial infection (Mayer-Barber and Barber, 2015).

Alveolar macrophages

When an animal is initially exposed to *M. bovis* by inhalation, the bacilli infect the AMs (Cooper, 2009) (Figure 2.1). The AMs are pulmonary resident macrophages that serve to clear alveoli of infectious particles (McClean and Tobin, 2016). The AMs can kill mycobacteria; however, bacilli can also escape the bactericidal effects of the AMs, usually when the host has impaired immunity or receives an overwhelming bacterial load (Cooper, 2009) (Figure 2.3). Bacterial evasion may occur by blocking of phagosome-lysosome fusion, resulting in reduced acidity of the phagosome and limited production of reactive oxygen species and nitrogen intermediates which are vital for the microbicidal activity of AMs (Ferguson *et al*., 2006).

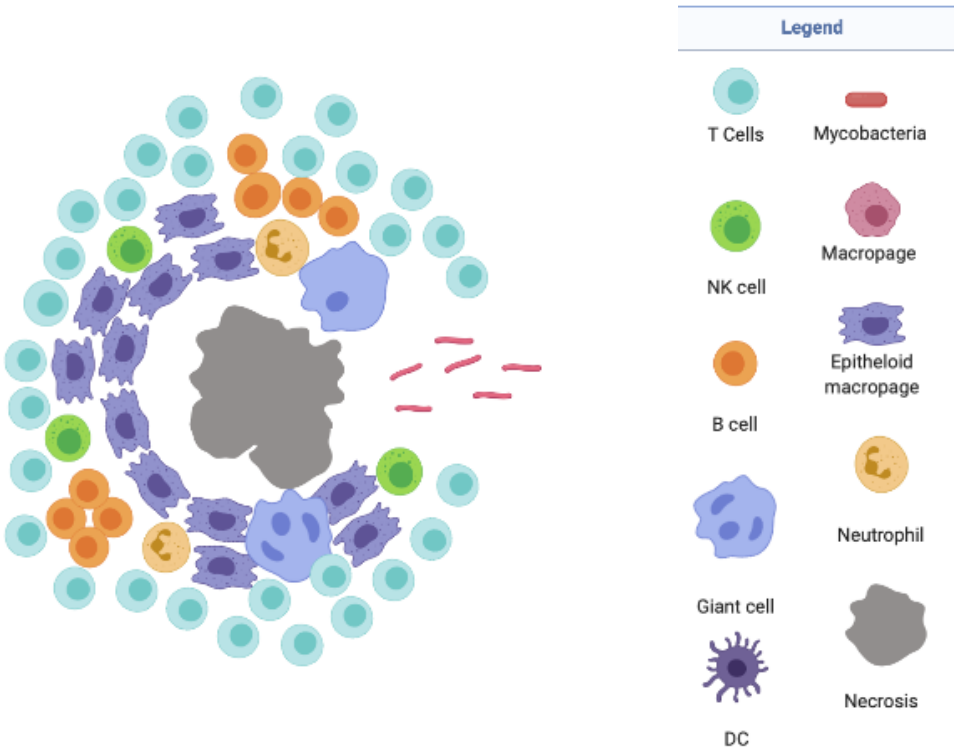

Figure 2.3. Illustration depicting an advanced tuberculous granuloma with a caseating, necrotic core and the escape of mycobacteria from the granuloma. Original figure designed with software at BioRender.com.

Epithelioid macrophages and multinucleated giant cells

The predominant cell type in a typical tuberculoid granuloma is the epithelioid macrophage (Palmer *et al.,* 2016) (Figure 2.2). Epithelioid macrophages have been characterised in early stages of granuloma development, however, relatively little is known about the specific signals that promote their participation in granuloma formation and maintenance (McClean and Tobin, 2016). Another type of macrophage, the MNGC is also present in the early stages of granuloma formation and has multiple nuclei organised at the periphery of the cytoplasm (Palmer *et al.,* 2016) (Figure 2.2). The development of MNGCs is not entirely understood but requires antigenic stimulation e.g. persistent mycobacteria (Anderson *et al.,* 2008). The function of MNGCs in granulomas is also poorly characterised, but in their absence, an ineffective immune response has been described (Palmer *et al.,* 2016). The MNGCs are often found where large or indigestible material is present, and therefore it is speculated that they are specialised for the uptake of large particles (Anderson *et al.,* 2008). The MNGCs produce various cytokines including tumor necrosis factor-alpha (TNF-α), interferon-gamma (IFN-γ), interleukin (IL)-10, transforming growth factor-beta (TGF-β) and the chemokines C-

C motif ligand (CCL)-2 and C-X-C motif ligand (CXCL)-10 (Mustafa *et al.,* 2006; Zhu *et al.,* 2012). Compared to epithelioid macrophages, MNGCs express more anti-inflammatory cytokines in response to *M. bovis* and have a higher antigen load and reduced bactericidal abilities (Mustafa *et al.,* 2008).

Natural killer cells and neutrophils

Other cells involved in innate immunity, such as NK cells and neutrophils, also participate in the early responses to mycobacterial infection in humans (Garand *et al.,* 2018) (Figure 2.1). Few studies have addressed the interaction between *M. bovis* and neutrophils (Jimbo *et al.,* 2017). Neutrophils are short-lived, however, the most abundant circulating leukocytes in many species (Lyadova, 2017). Neutrophils are the initial cells to arrive at the site of infection in a process facilitated by interactions between multiple neutrophil receptors (such as G-protein-coupled receptors (GPCR) and toll-like receptors) and microbial products, inflammatory cytokines and chemokines, and endothelial cell receptors (Lyadova, 2017). Neutrophils have phagocytic ability, however, information on the capacity of neutrophils to kill mycobacteria is conflicting (Lyadova, 2017). Several studies showed poor antimycobacterial activity of neutrophils, while other studies showed neutrophils were able to kill bacilli *in vitro* (Lyadova, 2017).

Natural killer cells produce IFN-γ, a potent pro-inflammatory cytokine important for the formation and maintenance of the granuloma (Esin and Batoni, 2015). In a study done by Denis *et al.* (2007), NK cells were stimulated by the release of IFN- γ and reduced *M. bovis* growth in infected macrophages. Natural killer cells also provide signals to infected AMs and DCs to assist with bacterial elimination by mediating cellular cytotoxicity (by releasing perforin and granulysin) (Garand *et al.,* 2008). The chemokines produced by the NK cells are important for the migration of immune cells to the site of infection. NK cells also display specific cell-surface memory-type markers to previous antigen exposure, thereby building a bridge between innate and adaptive immunity (Esin and Batoni, 2015).

Lymphocytes

After the DCs have phagocytosed the bacteria at the site of initial infection, they migrate to the lymph nodes to present mycobacterial antigens to T cells, initiating an adaptive response. Activation and recruitment of T cells to the site of infection trigger an intricate series of events, beginning with the T cells recognising specific peptides presented on major histocompatibility

complex (MHC) molecules resident on the membranes of various host cells (Wieczorek *et al.,* 2017). Antigens presented on MHC class I molecules, that occur on all nucleated cells, are recognised by cytotoxic CD8+ T cells (Wieczorek *et al.,* 2017). CD8+ T cells secrete granules containing cytotoxic molecules, such as perforin, granzymes, and granulysin that can lyse infected cells, as well as producing IFN-γ and TNF-α (El Fenniri *et al.,* 2011). These cytotoxic cells are also known to induce apoptosis of the infected cells through tumor necrosis factor-receptor (TNF-R) family-related cell-death receptors (El Fenniri *et al.,* 2011).

The CD4+ T cells recognise specific antigenic peptides as part of MHC class II complexes on antigen-presenting cells (APCs). Once activated, the CD4+ T cells, along with CD8+ T cells are recruited to the site of infection (Ulrichs *et al.,* 2004). The CD4+ T cells differentiate into various T-helper (Th) cell subsets including, but not limited to Th1, Th2, and Th17 cells (Cooper, 2009). Initially, most differentiated T cells will be in the Th1 subset. Th1 lymphocytes produce the cytokines IFN-γ and TNF-α which are essential for the initiation and maintenance of cell-mediated immune responses that eliminate intracellular mycobacteria (Kennedy *et al.,* 2002). Th1 and Th2 cells affect different cells and influence the type of immune response (Kennedy *et al.,* 2002). Th1 cells activate macrophages and participate in the generation of T cytotoxic cells. These T cells infiltrate the macrophage aggregates and eventually form a lymphocytic cuff around the macrophages and bacteria (Sasindran and Torrelles, 2019) (Figure 2.2). Th2 cells help activate B cells, resulting in antibody production hereby enhancing phagocytosis of the bacteria (Kennedy *et al.,* 2002; Sasindran and Torrelles, 2019).

It has been reported that B lymphocytes are present in clusters within the granuloma (Phuah *et al.,* 2012) (Figure 2.2). The role and function of B cells in TB granuloma formation are still unclear, but they are known to present TB antigens, and secrete cytokines and antibodies (Garand *et al.,* 2018). B cells are stimulated to become plasma cells which actively produce antibodies specific for TB antigens at the site of infection (Phuah *et al.,* 2012).

Cytokines

Cytokines are small proteins that mediate intercellular communication (Cavalcanti *et al.,* 2012) and in immune responses drive processes of both innate and adaptive immunity. Lymphocytes produce and secrete numerous vital cytokines that drive immune responses. The Th1 effector cells produce TNF-α, IFN-γ, and IL-2, important cytokines in the initial stages of granuloma

formation. These are critical pro-inflammatory cytokines that stimulate migration of immune cells to the site of infection, facilitate activation of macrophages and mediate the production of reactive nitrogen intermediates, which enhance the bactericidal function of macrophages (Cavalcanti *et al.,* 2012). The Th17 cell subset is characterised by the production of IL-17, a pro-inflammatory cytokine that has effects on epithelial, endothelial, and fibroblast cells (Tesmer *et al.,* 2012). The Th17 cells also respond to inflammatory signals in early infection and produce IL-1, a potent pro-inflammatory cytokine that has been shown to be involved in the control of mycobacterial infection (Fremond *et al.,* 2007). IL-1 is required for antigen-induced T cell proliferation and subsequently granuloma formation. In addition, IL-1 is responsible for signaling in the acute phase response (Fremond *et al.,* 2007). The production of the cytokine IL-12 by the DCs and macrophages is also vital for granuloma assembly (Cooper *et al.*, 1997).

As a granuloma matures, more Th2 cells begin to infiltrate the tissue. Th2 cells secrete B lymphocyte stimulating factors to promote the production of antibodies (Pagán and Ramakrishnan, 2018). The Th2 effector cells also produce the cytokines IL-4, IL-10, and IL-13, which contribute to pathogen sequestration, expulsion, and the healing of the lesion (Pagán and Ramakrishnan, 2018). IL-4 is considered a pleomorphic anti-inflammatory cytokine that drives the stimulation of antibody production and functions to counterbalance Th1 responses (de la Barrera *et al.,* 2004). The anti-inflammatory cytokines produced at the site of infection are important for balancing the inflammatory response and preventing excessive inflammation, thereby limiting immunopathological responses (de la Barrera *et al.,* 2004).

A deficiency or in some cases, a surplus of any of the cytokines involved in granuloma formation can result in disturbances in the development of these structures. For example, studies have shown a deficiency of TNF-α resulted in granulomas with increased influx of lymphocytes and neutrophils (Keane *et al.*, 2001). Such disturbances resulted in a disorganised granuloma, which was characterised by an absence of a lymphocytic cuff, no clear epithelioid macrophages, and MNGCs. A deficiency of IFN-γ also resulted in disorganised granuloma formation with an influx of neutrophils to the site of infection and decreased influx of lymphocytes (Pearl *et al.,* 2001). The production of the cytokine IL-12 by DCs and macrophages is also vital for granuloma assembly (Cooper *et al.*, 1997). A deficiency of IL-12 resulted in highly disorganised granulomas with decreased neutrophils and lymphocytes (Cooper *et al.*, 1997). An overproduction of IL-10 can result in disorganised granulomas with

increased macrophages and a decreased lymphocyte population, indicating the importance of anti-inflammatory, in addition to pro-inflammatory, cytokines in granuloma formation for the prevention of immunopathology (de la Barrera *et al.,* 2004).

Accessory features

During granuloma maturation, structural changes may occur that include fibrosis and necrosis, and can influence progression (Pagán and Ramakrishnan, 2008) (Figure 2.3). Fibrosis develops in response to the cytokines TGF-β, IL-13, structurally and functionally related pro-inflammatory cytokines, and the anti-inflammatory cytokine IL-4 (Pagán and Ramakrishnan, 2018). Fibrosis may be beneficial in terms of sequestering pathogens in the granuloma (Pagán and Ramakrishnan, 2018).

A granuloma with a caseous, necrotic center typically indicates a mature stage of development (Figure 2.3). Both necrosis and apoptosis of macrophages are observed in tuberculous granulomas. Central necrosis (caseous granulomas) is thought to be a result of death of macrophages and other participating cell types in granulomas (Ramakrishnan, 2012). Necrosis has been correlated with increased bacterial numbers and enhanced bacterial growth in macrophage-rich areas, as compared to non-caseous granulomas (Ramakrishnan, 2012). Necrotic granulomas usually contain multiple leukocyte populations, infected and uninfected macrophages, MNGCs and lymphocytes surrounding a necrotic core (Pagán and Ramakrishnan, 2018). This is typical in humans but differences in granuloma morphology may be seen in other animal species.

Granuloma developmental stages

Granulomatous lesions caused by *M. bovis* have been studied in cattle to investigate host mycobacterial growth control strategies for improving the understanding of disease pathogenesis (Carrisoza-Urbina *et al,* 2019). Although characterisation of granulomatous lesions in experimentally infected cattle has been reported, few studies have described stages of disease in naturally infected cattle (Carrisoza-Urbina *et al.,* 2019; Domingo *et al.,* 2014). Granulomas in cattle have been categorised into four different stages, all of which involve T cells (Wangoo *et al.*, 2005). There is an initial stage where irregular clusters of epithelioid macrophages are observed, with interspersed lymphocytes and small numbers of neutrophils. In some cases, MNGCs are present but there is no obvious necrosis. The second or "solid" stage consists of granulomas that are primarily composed of epithelioid macrophages enclosed

partly or entirely by a thin fibrous capsule. Haemorrhage is often observed with an infiltration of lymphocytes around the periphery of the central macrophages and minimal necrosis is observed. In stage three or the "minimal necrosis" stage, granulomas are encapsulated by a fibrous capsule, with central caseous necrosis and some mineralisation present. Domingo (2014) found minimal mineralisation in granulomas during this stage. Epithelioid macrophages are abundant among MNGCs surrounding an area of central necrosis. Peripherally, clusters of lymphocytes and scattered neutrophils extend into the fibrous capsule. The fourth and final stage, is characterised by granulomas that are thickly encapsulated by a fibrous capsule and large, irregular and multicentric caseous necrosis (Wangoo *et al.*, 2005). Extensive mineralisation is also typically present. Acid-fast bacilli are present extracellularly within the necrotic caesium and rarely within macrophages or MNGCs (Palmer *et al.*, 2007). Different developmental stages of granuloma formation can also be found within the same animal and same tissue (Carrisoza-Urbina *et al,* 2019). As is typical for most MTBC organisms, very low numbers of acid-fast bacteria may be found within the caseous material or within epithelioid cells or MNGCs in most bTB lesions (Domingo, 2014). In a study by Carrisoza-Urbina *et al.* (2019), a predominance of stage four granulomas was found in naturally infected cattle, suggesting a chronic process possibly involving an imbalance in immune processes.

Species Differences in bTB Lesions

Due to its broad host range, *M. bovis* can readily spillover from cattle into other animal species including wildlife. Once the disease becomes endemic in wildlife populations, disease control is a serious challenge (Fitzgerald and Kaneene, 2012). There are many animal reservoirs for bTB globally, each showing some differences in pathology. In general, typical granulomas of bTB are similar to those of human tuberculosis, although the latter is caused by infection with *M. tuberculosis.* Differences in lesion morphology may be attributed to both differences in offending pathogens and host responses (Palmer *et al.,* 2018).

Ruminants

The pathologic changes associated with bTB have been described in greater detail in cattle compared to other animal hosts. The typical gross lesion of *M. bovis* in cattle, known as a tubercle, has been characterised in studies of natural and experimental infections (Domingo *et al.,* 2014). The route of transmission may determine the location and spectrum of the lesions observed. Aerosol transmission is the most common form of transmission of *M. bovis* in cattle and results in granulomas in the nasopharynx, the lower respiratory tract, and

the associated lymph nodes (Domingo *et al.,* 2014). Granulomas are circumscribed yellowish masses, about 2-20mm in diameter, generally encapsulated by connective tissue and often contain mineralisation (Domingo *et al.,* 2014). In cattle, lesions have been microscopically classified into four categories (Menin *et al.,* 2013), which have been described above.

African buffaloes (*Syncerus caffer*) are regarded as a maintenance host for *M. bovis* in South Africa (Tadayon *et al.,* 2006). Previous reports of *M. bovis* in buffalo have shown lesions occur predominantly in the head and thoracic lymph nodes, and in the tonsils and lungs (Laisse *et al.,* 2015). Infected lymph nodes can become enlarged and contain lesions of variable size with central areas of caseation, mineralisation, necrosis, and fibrous encapsulation (Laisse *et al.,* 2015). Infected lymph nodes in buffaloes contained granulomas which may have both caseous necrotic and mineralised cores. In the lungs, lesions are either disseminated or present as individual granulomas (Laisse *et al.,* 2015). Histologically, bTB lesions in buffalo contain a variety of inflammatory cells including macrophages, MNGCs, and lymphocytes (Laisse *et al.,* 2015). In the study by Laisse *et al.* (2015), the granulomas were classified into four categories, namely stage I (initial or early lesions); stage II (solid granulomas), stage III (minimal necrosis), and stage IV (necrosis and mineralization). This classification is similar to that described for human TB granulomas, as well as those in domestic cattle.

Other ruminants including cervids are common hosts affected by bTB. In a study by Johnson *et al.* (2007), bTB granulomas in British deer, which included red deer (*Cervus elaphus*) and fallow deer (*Dama dama*), were assessed using immunohistochemical techniques. These animals were believed to have been exposed to *M. bovis* by aerosol transmission and had lesions like those described in humans and bovids. Generally, most lymph node granulomas in the deer were necrotic and encapsulated, while lung granulomas possessed no fibrous capsule (Johnson *et al.,* 2007). In a study on white-tailed deer (*Odocoileus virginanus*) in the United States, bTB granulomas were similar to those in the deer studied in the U.K; lesions often grossly resembled abscesses due to a soft caseous core (Fitzgerald and Kaneene, 2012).

Although the general pathologic features of bTB in cattle are shared with most other species, there have been some differences in types and distributions of lesions (Domingo *et al.,* 2014). Caprine tuberculosis, resulting from *Mycobacterium caprae* or *M. bovis* infection in goats, displays cavitary lesions with bacterial growth in addition to the typical tuberculoid granulomas found in the lungs and lymph nodes (Sanchez *et al.,* 2010). Differences have been noted

between granulomata and cavitary lesions. Cavitary lesions or "open lesions" have a substantial population of neutrophils and fewer CD4+ T cells, with an increase in other T cell populations including CD8+ T cells (Sanchez *et al.,* 2010). In addition, cavitary lesions contained large amounts of the enzyme iNOS (inducible nitric oxide synthase), which provides bactericidal activity of macrophages towards bacilli (Sanchez *et al.,* 2010). The cavitary lesions appear to be optimal sites for mycobacterial proliferation. Other more typical granulomatous lesions have also been reported in goats with central areas of necrosis surrounded by macrophages, epithelioid cells, MNGCs, and lymphocytes (Sanchez *et al.,* 2010).

Suids

Infection in cattle and wildlife may be linked to the spillover of bTB into other species including domestic pigs and wild boar (*Sus scrofa*) (Bailey *et al.,* 2013). Although the European wild boar is frequently considered a spillover host, studies from Mediterranean Spain have demonstrated that the species can also serve as a reservoir host (Naranjo *et al.,* 2007). Evidence supporting this includes the sharing of common MTBC genotypes in wild boar, domestic and wild animals, and humans; high prevalence of *M. bovis* among wild boar fenced off for decades from domestic livestock; TB lesions often seen in the thoracic lymph nodes and lungs, suggesting respiratory transmission, and lesions in multiple anatomical sites in juvenile wild boars (Naranjo *et al.,* 2007).

The oral route of infection is common in swine and therefore lesions are frequently found in the oropharyngeal lymph nodes, the gastrointestinal tract, as well as the mesenteric and portal lymph nodes (Domingo *et al.,* 2014). In addition, infected wild boars may have lesions in the lungs, liver, and spleen (Fitzgerald and Kaneene, 2012). Bailey *et al.* (2013) described the gross appearance of lesions due to *M. bovis* infection in pigs as white-yellow, calcified, often encapsulated granulomas, mainly in the lymph nodes of the head. Lesions in pigs can also be more disseminated than those observed in cattle, with less necrosis and mineralisation (Domingo *et al.,* 2014).

Badgers

In the United Kingdom, the European badger (*Meles meles*) is a reservoir species for bTB (Gormley and Corner, 2018). The pathogenesis of bTB in naturally infected badgers has been studied extensively (Gormley and Corner, 2018). In badgers, the typical route of infection is by inhalation of infectious aerosols, resulting in lesions in the thoracic lymph nodes and lungs

(Gormley and Corner, 2018). Granulomas are composed of macrophages and few lymphocytes, and are typically proliferative with limited necrosis, mineralization, or fibrosis (Gormley and Corner, 2018). As areas of central necrosis increase, the number of bacilli present increases. Subsequently, as the severity and size of lesions increase, the central mass of epithelioid cells also increases and is enclosed by a rim of lymphocytes with an outer layer of macrophages and neutrophils bound by a fibroblast layer (Gormley and Corner, 2018). A second route of infection associated with contamination of bite wounds has also been recognised. Lesions containing *M. bovis* in bite wounds develop circumscribed subcutaneous granulomas, which can progress to draining abscesses and large open ulcerated areas devoid of skin (Gormley and Corner, 2018).

Brushtail Possum

The brushtail possum (*Trichosurus vulpecula*), another reservoir host, is native to Australia and Tasmania, and was introduced to New Zealand in the mid-1800s (Fitzgerald and Kaneene, 2012). Possums are highly susceptible to *M. bovis* infection and typical gross lesions include multifocal granulomatous lymphadenitis. Granulomas have necrosis with mineralisation and fibrosis is rarely observed (Nugent *et al.,* 2015). Inflammatory infiltrates consist of macrophages, lymphocytes, and neutrophils, interspersed with MNGCs. Lesions are generally disseminated, affecting multiple tissues (Nugent *et al.,* 2015).

Felids

Although carnivores are generally thought to be more resistant to infection, both wild and domestic felids have been reported with bTB. In 1998, *M. bovis* was detected in two snow leopards (*Panthera unica*) in the Tulsa Zoological Park (Helman *et al.,* 1998). Infection was pulmonary and characterised by typical organised granulomatous inflammation (Helman *et al.,* 1998). In lions, pulmonary lesions are absent in early infection (Keet and Meltzer, 1998). Infection is believed to occur orally due to the consumption of infected prey, although social and intra-species aggression between lions can expose them to aerosol transmission (Michel *et al.,* 2006). Tuberculosis lesions in lions differ macroscopically from those described in non-human primates and ungulates (Viljoen *et al.,* 2015). Pulmonary lesions in lions tend to be cavitary, without mineralisation and liquefactive necrosis (Viljoen *et al.,* 2015). Lymph node granulomas showed extensive fibrosis and slight focal necrosis, and histologically consisted of macrophages (including epithelioid), lymphocytes, and neutrophils

(Viljoen *et al.,* 2015). Because lesions in felids have often lacked caseation, they can resemble neoplastic processes (Domingo *et al.,* 2014).

The occurrence of TB in domestic cats has been increasingly recognized (Gunn-Moore, 2014). Cats may have been bitten by *M. bovis*-infected small rodents or exposed to environmental contamination (Gunn-Moore, 2014). In domestic cats, infections are typically cutaneous with lymphadenopathy (Gunn-Moore, 2014). Skin lesions may be single or multiple raised nodules which may or may not be ulcerated and can have associated draining sinus tracts (Gunn-Moore, 2014). In animals with chronic disease, dissemination of infection to the lungs may occur (Gunn-Moore, 2014).

Conclusion

Regardless of species, granulomatous inflammation or granulomas are the hallmark lesion of TB. In recent years, there has been an increase in information regarding granuloma formation, structure and function, especially in humans and cattle. Generally, lesions caused by *M. tb* and *M. bovis* have similar appearance and structure. However, the presentation of *M. bovis*-associated disease can vary between species and the route of infection. In cattle, granulomas have been categorised into four groups based on lesion development, which have been linked to the progression of disease (Wangoo *et al.,* 2005). Findings suggest that host responses and the resulting pathological changes in *M. bovis*-associated disease are dynamic processes with the immune cell populations and pathogen distribution changing over time. Further investigation to better understand pathogenesis is warranted. Importantly, TB lesions have not been fully characterised in wildlife and given the impact this disease may have on conservation, it is imperative to characterise the host-pathogen responses associated with *M. bovis* infection in non-domestic species as well.

Chapter 3: Materials and Methods

Ethical and regulatory approval

Ethical approval for this study was granted by the University of Stellenbosch Animal Care and Use Committee (ACU-2019-9081). Section 20 approval was granted by the Department of Agriculture, Forestry and Fisheries, South Africa (DAFF; 12/11/1/7/2).

Study site and animals

Samples were collected from buffaloes captured during the 2018 and 2019 annual bTB test-and-slaughter program in Hluhluwe-iMfolozi (HiP) Game Reserve, a *M. bovis* endemic area of northern KwaZulu Natal, South Africa (Parsons *et al.,* 2011). Cytokine release assays, including the modified QuantiFERON TB-Gold interferon gamma release assay (QFT IGRA) (Qiagen, Johannesburg, South Africa), the in-house bovine interferon gamma-induced protein 10kDa release assay (QFT IPRA), and single intradermal comparative tuberculin test (SICTT) were performed to evaluate *M. bovis* immune sensitisation in all buffaloes as previously described (Bernitz *et al.,* 2018; Smith *et al.,* 2021). Any individual buffalo that had at least one positive test result (Appendix 1) was culled and examined for gross bTB lesions at necropsy (Smith *et al.,* 2021). In 2018, a whole herd was culled during the test-and-slaughter program due to high bTB prevalence in the herd.

Post-mortem examination and mycobacterial culture

Gross pathologic changes in buffalo lung samples consistent with bTB lesions were discrete, caseous or calcified, yellowish nodular foci interpreted as consistent with granulomas (Laisse *et al.,* 2010). Lesions were scored at necropsy by the same experienced veterinarian as follows: 0, no visible lesions; 1, one small (< 10 mm in diameter) focal lesion; 2, several small focal (more than 1 lesion < 10 mm in diameter) or single large (> 10 mm in diameter) lesion; and 3, multifocal or confluent lesions, based on a system described in cattle (Palmer *et al*., 2007). Lung samples with bTB-like lesions were collected and stored separately in sterile tissue containers. Lung tissue samples were split into thirds, with two samples frozen at -20°C, and another section placed in 10% buffered formalin (Kimix Chemicals, Cape Town, South Africa). In addition, cattle lung samples, from three apparently healthy animals from *M. bovis*-free herds, were obtained from an abattoir in Malmesbury, South Africa, to use as control tissues to assess the cross-species reactivity of the antibodies used in IHC analysis. The cattle lung tissues were cut in half, with one half placed in 10% buffered formalin and half placed in

dibutylphtalate polystyrene xylene (DPX) mounting media, (Sigma-Aldrich^{TM,} Cape Town, South Africa) prior to freezing at -20°C.

One set of frozen lung samples from culled buffaloes was processed for mycobacterial culture. Tissues were processed in at the BSL-3 facility, Stellenbosch University, South Africa and then cultured using the Mycobacterial Growth Indicator Tube (MGIT^{TM}) (BACTEC^{TM}, New Jersey, United States) system, as described by Goosen *et al.* (2014). Genetic speciation by PCR of cultured isolates was performed and used to confirm the presence of *M. bovis* as previously described (Hilleman *et al.,* 2006; Goosen *et al.,* 2014).

Histopathology

For histopathologic examination, lung samples were chosen from buffaloes that had gross lesion scores of 1, 2 or 3. Buffalo tissues collected in HiP in 2018 that had been stored in 10% buffered formalin (Kimix Chemicals) for more than a year were used for histopathologic analysis. For each selected buffalo sample, a single representative section was selected for light microscopy. The buffalo and cattle tissues that were stored in 10% buffered formalin (Kimix Chemicals) were dehydrated using a series of ethanol solutions (1x 70% ethanol, 2x 96% ethanol and 2x 99.9% ethanol) (Kimix Chemicals) and cleared in xylene (2x) (Kimix Chemicals), then embedded in paraffin wax at 60℃ using the Leica EG1160 embedder (SMM Instruments, Midrand, Gauteng, South Africa). The portion of each tissue with visible lesions was selected for paraffin embedding using an automated tissue processor. Wax embedded tissues were kept at 20-25°C and then sectioned using a microtome (Leica® RM2125RT, Cape Town, Western Cape, South Africa). Frozen cattle tissues were sectioned using the Cryostat apparatus (Leica® CM1850). Tissue sections were cut to 4-5 µm thickness, then stained with haematoxylin and eosin (H&E) (Appendix 2) for general morphologic evaluation. The basic dye, haematoxylin, stains basophilic structures such as nuclei, ribosomes and the rough endoplasmic reticulum purple (Fischer *et al.,* 2006). In contrast the acidic dye, eosin, stains eosinophilic structures, such as cytoplasmic proteins, red (Fischer *et al.,* 2006). Serial sections, approximately 5 µm thick, were prepared and stained with Ziehl-Neelsen (ZN) to assess the presence of acid-fast bacilli (Appendix 3).

Image analysis of H&E stained tissue sections

The H&E stained lung sections were examined using an Axiolab 5 light microscope with the Axiolab 208 color camera (Zeiss, Cape Town, Western Cape, South Africa) and the ZEISS Efficient Navigation (ZEN) ^{TM} microscope software, version 2 Lite (Zeiss). The H&E stained

buffalo lung sections were scanned using the Aperio ScanScope CS whole slide scanner (Aperio, Virginia, USA) at 40x magnification, with a resolution of 0.25 /pixel. QuPath version 0.2.3 software (Queen's University, Belfast, Ireland) was used to visualise and capture images of the tissue sections. Sections were evaluated to characterise overall morphologic and specific histologic features were scored by a single examiner (S. Goldswain); the scoring criteria were developed in consultation with an American College of Veterinary Pathologists (ACVP) board certified pathologist (J. Landolfi). Each slide was scanned, and the numbers of discrete granulomas were recorded for the entire tissue section on each slide. If a granuloma was incomplete (extended off the slide), the lesion was recorded as half. If a lung section had a single granuloma, the granuloma was used for scoring the slide. However, if multiple granulomas were present in a single section, all the granulomas were scored. The sub gross appearance of the granulomas was noted based on whether a granuloma(s) was present, focal or multiple, and separate or coalescing. Granulomas were scored, based on the six categories shown in Table 3.1, to provide a semi-quantitative description of buffalo pulmonary granulomas.

Table 3.1. Criteria for scoring microscopic characteristics of buffalo pulmonary granulomas (based on a single slide) using values ranging from 0-3.

	Score 0	Score 1	Score 2	Score 3
Necrosis score	0% of the granuloma was necrotic	<25% of the granuloma was necrotic	25-50% of the granuloma was necrotic	>50% of the granuloma was necrotic
MNGC score	No MNGCs present	Less than 10 MNGCs present	Between 10-25 MNGCs present	More than 25 MNGCs present
Lymphocyte infiltration score	No lymphocytes infiltrating the granuloma	Few lymphocytes infiltrating the granuloma	Moderate numbers of lymphocytes infiltrating the granuloma	High numbers of lymphocytes infiltrating the granuloma
Mineralisation score	No mineralisation present	Mineralisation present	Not applicable	Not applicable
Fibrous encapsulation score	No fibrous capsule surrounding the granuloma	Thin fibrous capsule surrounding the granuloma	Moderate fibrous capsule surrounding the granuloma	Thick fibrous capsule surrounding the granuloma
Total tissue destruction score	No tissue replaced by granulomatous inflammation	<25% of the tissue replaced by granulomatous inflammation	25-50% of the tissue replaced by granulomatous inflammation	>50% of the tissue replaced by granulomatous inflammation

MNGCs – multinucleated giant cells

The six granuloma characteristics scored in categories were as follows:

1. Necrotic area score: The necrotic area score of each granuloma in the buffalo lung section was based on the estimated percentage of the total granuloma that was necrotic, with scores ranging from 0 (i.e. no necrosis) to 3 (i.e. greatest amount of necrosis). Criteria are shown in Table 3.1 and the images of examples of granulomas with differing scores are presented in Figure 3.1a-d.

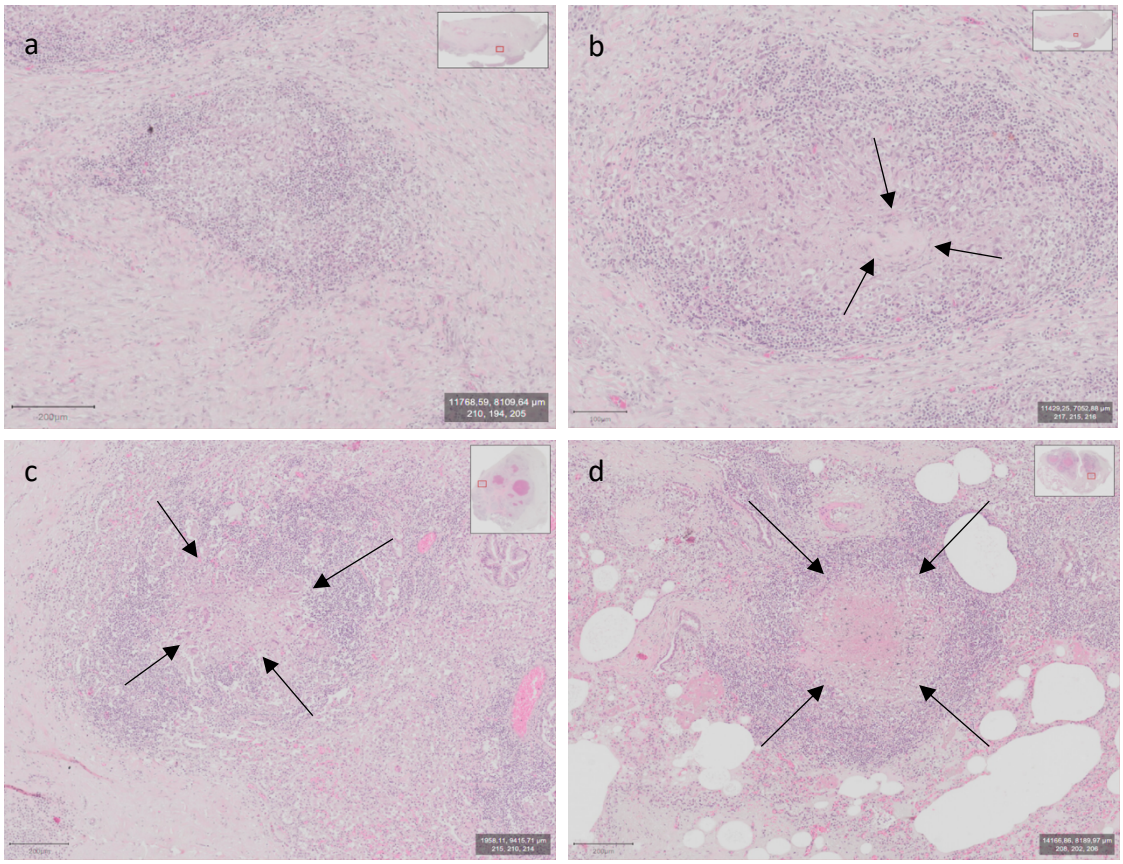

Figure 3.1. Photomicrograph of the necrosis in a granuloma in a H&E section of buffalo lung tissue at 40x magnification, presented at a resolution of 3.8x; (a) showing examples of 0% necrosis in granuloma; (b) <25% of granuloma as necrotic; (c) 25-50% of granuloma as necrotic; (d) and > 50% of granuloma as necrotic as indicated by the arrows.

2. Multinucleated giant cell (MNGC) score: The MNCG score was based on number of MNGCs present in each granuloma using the scoring criteria shown in Table 3.1. An example of the microscopic appearance of a MNGC in a buffalo pulmonary granuloma is shown in Figure 3.2.

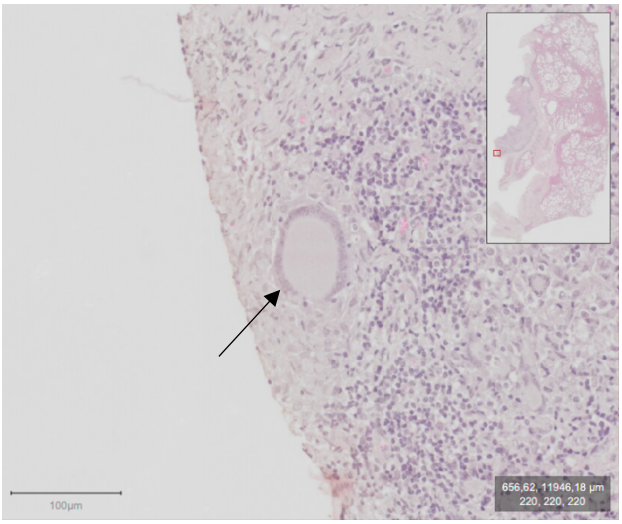

Figure 3.2. Photomicrograph of H&E stained buffalo lung tissue section, scanned at 40x magnification, showing the appearance of a typical MNGC (indicated by the arrow; presented at a resolution of 5.7x).

3. Microscopic score for lymphocytic infiltration in each granuloma: This score was based on a subjective assessment of the relative number of lymphocytes associated with the granuloma, based on the criteria shown in Table 3.1. The appearance of a typical lymphocyte in a buffalo pulmonary granuloma is shown in Figure 3.3a; examples of varying degrees of lymphocyte infiltration are shown in Figure 3.3b-d.

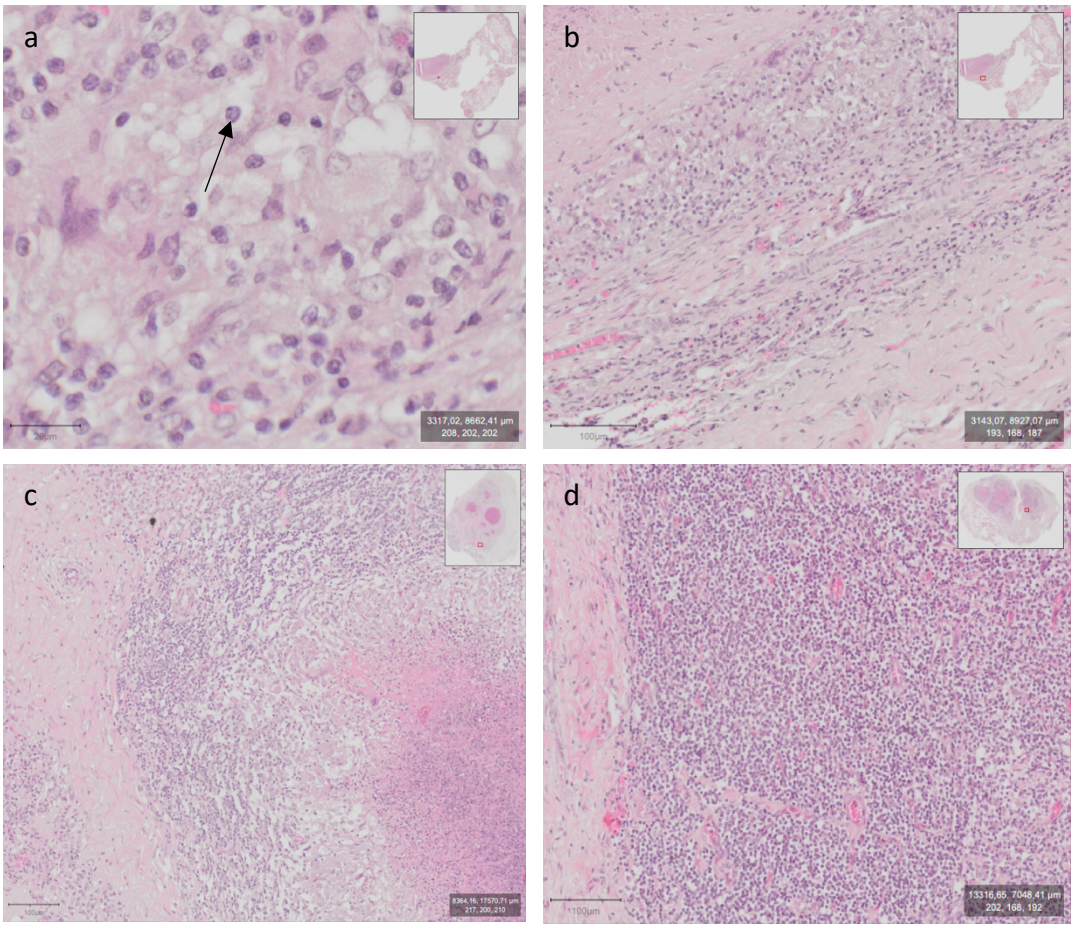

Figure 3.3. Photomicrographs of H&E stained buffalo lung tissue sections, scanned at 40x magnification: (a) shows the appearance of a typical lymphocyte (arrow) in H&E stained buffalo tissue, with arrow indicating a lymphocyte, presented at a resolution of 20x. Examples of tissue sections showing differing numbers (scores) of lymphocytes infiltrating the granuloma, presented at a resolution of 6.8x; (b) lymphocytic infiltration score 1, low numbers of lymphocytes; (c) lymphocytic infiltration score 2, moderate numbers of lymphocytes; (d) lymphocytic infiltration score 3, high numbers of lymphocytes.

4. Microscopic mineralisation scores for granulomas were assigned based on the presence or absence of visible mineralisation within the granuloma (usually centrally located) in each slide. Criteria for the scores (0 or 1) are shown in Table. 3.1, and examples of granulomas without and with mineralisation are presented in Figure 3.4a and b.

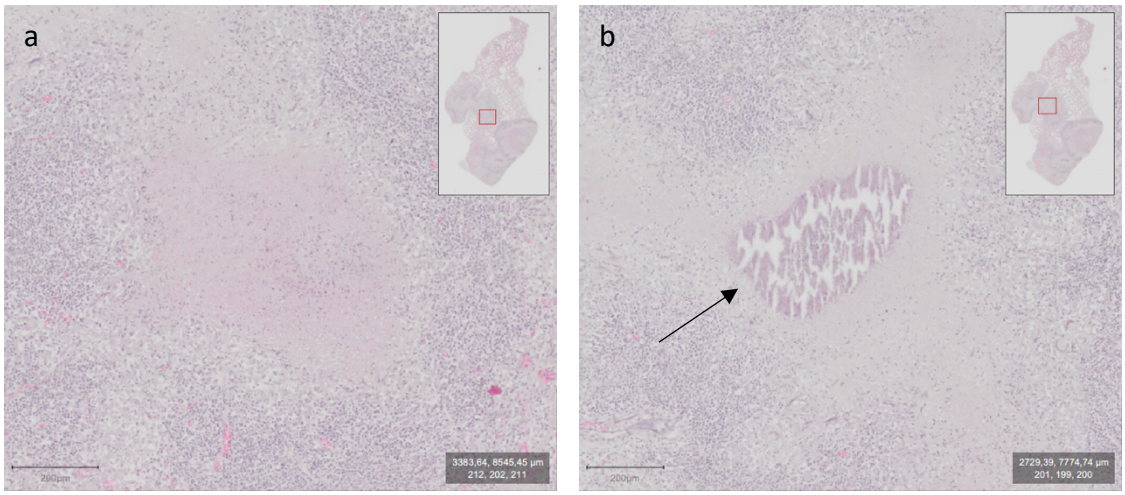

Figure 3.4. Photomicrograph of H&E stained buffalo lung tissue sections, scanned at 40x magnification, presented at a resolution of 3.7x. Examples of differing mineralisation scores: (a) mineralisation score 0 – granuloma without mineralisation; (b) mineralisation score 1 - granulomas with mineralisation present. The arrow indicates the area with visible mineralisation.

5. Microscopic score for fibrous encapsulation of each granuloma in each slide was based on the subjective assessment of the presence and amount of fibrous tissue at the periphery of the granuloma. The criteria for these scores (ranging from 0 to 3) are shown in Table 3.1. An example of a fibroblast in a buffalo pulmonary granuloma is seen in Figure 3.5a and examples of differing thickness of fibrous capsules are presented in Figure 3.5b-d.

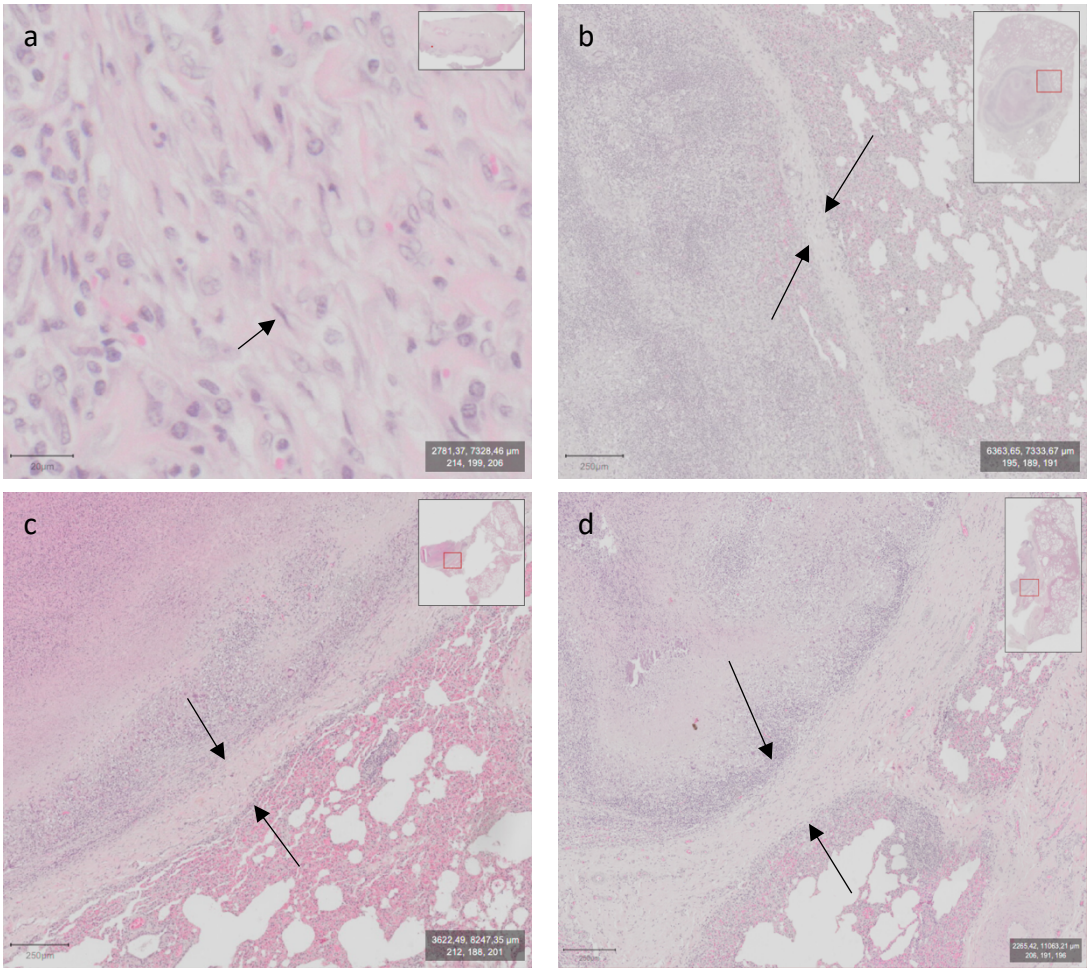

Figure 3.5. Photomicrographs of H&E stained sections of buffalo lung tissue sections, scanned at 40x magnification: (a) shows the appearance of a typical fibroblast cell in H&E stained buffalo tissue, indicated by the arrow (presented at a resolution of 17.6x). Examples of the different fibrous capsule scores, presented at a resolution of 2.5x: (b) score 1 - a thin fibrosis capsule surrounding the granuloma; (c) score 2 – moderately thick fibrosis capsule surrounding the granuloma and (d) score 3 - thick fibrous capsule surrounding the granuloma. Arrows indicated the fibrotic capsule in each example.

6. Microscopic score for estimated amount of lung tissue replaced/distorted by granulomatous inflammation in each tissue section was based on the subjective assessment of the area of the tissue section comprised of the granulomas, using the criteria in Table 3.1. Examples of differing degrees of tissue replacement are presented in Figure 3.6a-c.

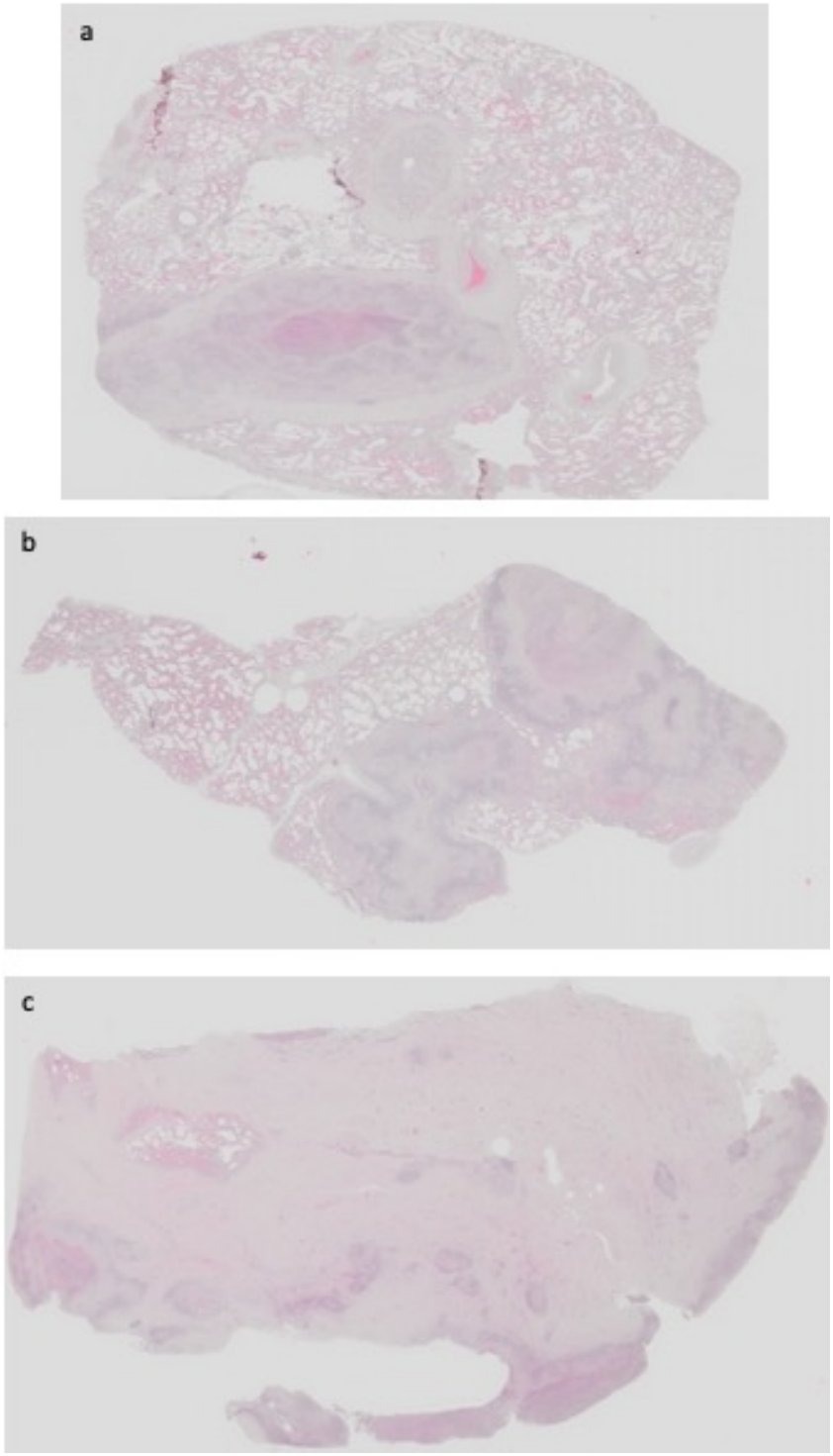

Figure 3.6. Photomicrographs of H&E stained sections of buffalo lung tissue sections scanned at 40x magnification. Examples of the different total tissue destruction scores (presented at a resolution of 0.25x): (a) score 1 - less than 25% of the tissue is replaced by granulomatous inflammation; (b) score 2 – 25-50% of the tissue is replaced by granulomatous inflammation and (c) score 3 - greater than 50% of tissue is replaced by granulomatous inflammation.

Staging of buffalo lung granulomas

After visual evaluation of the histopathological changes in the lung tissue, each buffalo lung tissue section was assigned to one of four granuloma developmental stages, shown in Table 3.2. Descriptions of granulomas were adapted from the system for cattle bTB lesions as described by Wangoo *et al.* (2005). The criteria for the scoring system applied was adapted from the grading system of canine mammary tumors described by Goldschmidt *et al.* (2011). The scoring data for all the buffalo lung granulomas in a section were collated in an Excel version 16.29 (2019, Microsoft, Redmond, Washington, USA) spreadsheet, and the granulomas were assigned a stage based on a sum of all the microscopic scoring criteria described above and a numerical range of each of the granuloma stage assignments; stage I = 3-5; stage II = 6-7; stage III = 8-9; and stage IV = ≥ 10.

Table 3.2. Criteria used to assign stages (I-IV) of granuloma development in lung samples from *M. bovis*-infected buffalo.

Description	Total score	Allocated stage
Initial granuloma – irregular clusters of macrophages and MNGCs interspersed with lymphocytes; no necrosis and fibrosis.	3 to 5	Stage I
Early granuloma –macrophages and MNGCs dominate, with interspersed lymphocytes; thin or incomplete fibrous capsule; minimal central necrosis or haemorrhage.	6 to 7	Stage II
Development of a necrotic core – macrophages and MNGCs surround area of necrosis, lymphocytes located peripherally; complete fibrous encapsulation and central necrosis often with mineralisation.	8 to 9	Stage III
Advanced granuloma - macrophages and MNGCs surround area of necrosis, lymphocytes are prominent; thick fibrous encapsulation and multicentric caseous necrosis with mineralisation.	10 or above	Stage IV

Immunohistochemistry (IHC)

Protocol optimisation

Washington State University (WSU) monoclonal antibodies

Serial tissue sections from buffalo lung samples, prepared as described above, were processed for immunohistochemistry. Sections were taken from each tissue sequentially to the H&E sections to maintain consistency between H&E and IHC sections as much as possible. Monoclonal, bovine-specific antibodies for immune surface markers listed in Table 3.3 were obtained from the Monoclonal Antibody Center of Washington State University (Pullman, WA, USA).

Table 3.3. Specifications of the Washington State University monoclonal primary antibodies used to stain buffalo lung tissues.

Antibody (cell surface marker)	Description	Isotype	Specificity	Catalog #	Host species	Concentration (mg/ml)	Storage temperature (°C)
CD3	Monoclonal	IgG1	Bovine pan T Cell	MM1A	Mice	1.0	2-7
CD4		IgM	Bovine CD4 T Cell	CACT83B			
CD8		IgM	Bovine CD8 T cell	BAQ11A			
CD21		IgG1	Bovine B Cell	GB25A			
CD163		IgG1	Bovine macrophage	LND68A			
CD335		IgG1	Bovine natural Killer	EC1.1			
MM20A		IgG1	Bovine neutrophil	MM20A			

An overview of the optimisation process is displayed in Figure 3.7. Each WSU antibody was tested on buffalo lung tissue sections that had been fixed in 10% buffered formalin for over a year; buffalo lung tissue that had been frozen for the same amount of time was thawed and placed in 10% buffered formalin for 48 hours prior to sectioning. Cattle lung tissues that had been frozen; and cattle lung tissue that had been fixed in formalin for 48 hours prior to processing were used as negative controls.

Abcam beta actin antibody control

To determine the degree to which formalin fixation (one year or 48 hours) impacted the tissue integrity and antibody binding ability and ensure the success of the staining protocol, an anti-

beta actin antibody (ab8227, Abcam, Cape Town, South Africa) was included as a positive staining control. The anti-beta actin antibody was tested on the same tissues described above. An additional section of each tissue was used as a negative control, by processing it in parallel, but without including the primary antibody.

Experimental sample evaluation

An alternate set of antibodies (Abcam; Table 3.4), was used to stain tissue sections from previously frozen, formalin-fixed buffalo lung samples. A Leica Bond-III Fully Automated IHC Stainer^{TM} (Leica Biosystems) was used for staining buffalo lung tissues. Sections were dewaxed, deparaffinized and rehydrated using fresh xylene and a graded ethanol series (2x 99.9%, 2x 96%, 1x 70%). Slides were subsequently soaked in Peroxide Block (3-4% hydrogen peroxide), from the Refine Detection Kit for 5 minutes (Leica Biosystems), and then in methanol (Kimix Chemicals) for 15 minutes to eliminate any endogenous peroxidase activity. Antigen retrieval was performed by incubating slides for 20 minutes in citric acid buffer at 100°C (pH 6; epitope retrieval solution 1) (Leica Biosystems) or for 20 minutes by heat mediated antigen retrieval using EDTA at 100°C (pH 9; epitope retrieval solution 2) (Leica Biosystems). The tissues were stained with bovine IgG primary antibodies (Table 3.4) for 30 minutes.

Table 3.4 Details pertaining to the Abcam antibodies including their isotype, specificity, catalog number, host species to which antibodies were originally raised, concentration and storage temperature.

Antibody (cell surface marker)	Description	Isotype	Specificity	Catalog #	Host species	Concentration (mg/ml)	Storage temperature (°C)
CD3	Monoclonal	IgG	Pan T Cell	Ab16669	Rabbit	1.0	4
CD4			CD4 T Cell	Ab133616			
CD21			B cell	Ab75985			
CD163			Macrophage	Ab182422			
NCR1			Natural Killer Cell	Ab233558			
Beta actin	Polyclonal		Beta actin	Ab8227			

Sections were washed with BOND^{TM} wash solution (Leica Biosystems) twice for three minutes. Sections were then incubated with the appropriate post primary rabbit anti-mouse IgG antibody (10 ug/ml) (Leica Biosystems) for eight minutes, before being washed again, and incubated with poly-horseradish peroxidase (HRP) IgG reagent (Leica Biosystems) for eight minutes. Antibody binding was detected using 3,3'-diaminobenzidine tetrahydrochloride (DAB; Leica Biosystems) and finally sections were counterstained with haematoxylin for five minutes (Leica Biosystems), dehydrated and cleared in fresh xylene before being mounted with DPX (Sigma-Aldrich) and covered with coverslips (Kimix Chemicals). A replicate section from each tissue was included as a negative control and run in parallel with the other sections, but without the primary antibody antibodies.

Image analysis of IHC stained tissue

To investigate the staining patterns of immune cell surface markers in buffalo pulmonary granulomas, antibody stained tissue sections were scanned using the Aperio ScanScope CS whole slide scanner (Aperio, Virginia, USA) at 40x magnification, with a resolution of 0.25/pixel. QuPath v 0.2.3 software (Queen's University, Belfast, Ireland) was used to visualize the tissue sections, capture images, and to assess the staining patterns of the beta actin, CD4 and CD3 (T lymphocytes), CD21 (B lymphocytes), NCR1 (NK cells) and CD163 (macrophages) positive cells in buffalo lung granulomas.

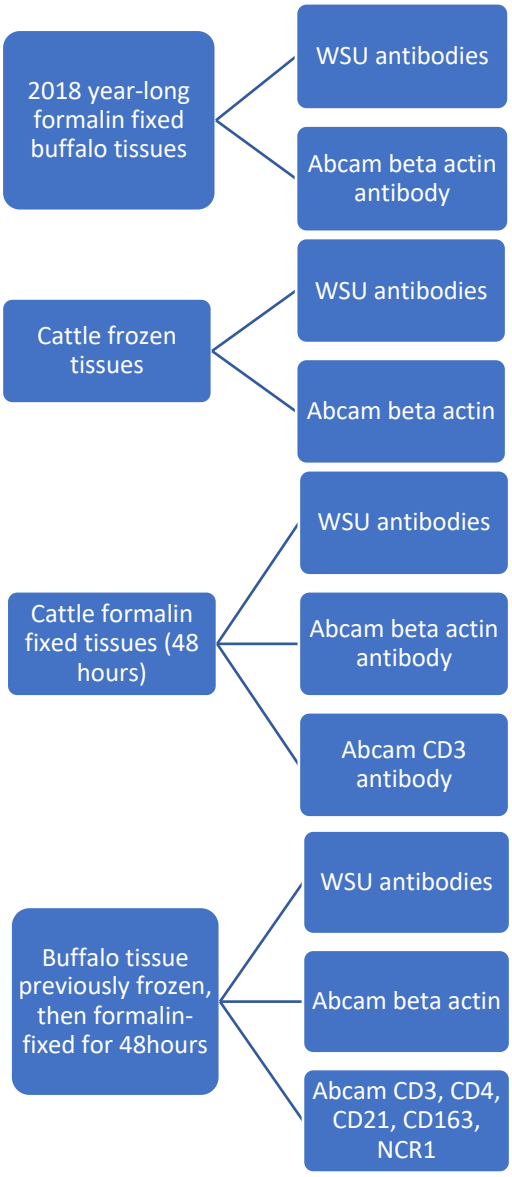

Figure 3.7. Flow diagram showing the different cattle and buffalo tissues used in the process of optimising the immunohistochemistry protocol with the different antibodies tested.

Chapter 4: Results

Histopathology

Lung samples from 12 buffaloes were selected for histologic evaluation based on their positive *M. bovis* culture result. The details of additional test results on these buffaloes are included in Appendix 1. Upon gross examination, one tissue had a gross score of 0, three tissues had a gross lesion score of 1, four had a gross lesion score of 2, and six had a gross lesion score of 3. Examples of gross lesions in buffalo lung tissue samples are shown in Figure 4.1.

Figure 4.1. Photographs taken during post-mortem examination showing examples of (a): small focal lesions in a section of buffalo lung tissue taken from a calf as indicated by the arrow; and (b) a large, caseating lesion in the lung of an adult buffalo (buffalo 14).

The microscopic appearance of the buffalo lung tissue sections was evaluated for the presence of granulomas and a score assigned for the amount of total tissue destruction in the slide (Table 4.1). Of the 12 lung samples examined, 9 had granulomas that showed typical characteristics associated with bTB granulomas, i.e. central necrosis with an infiltration of macrophages and lymphocytes forming a lymphocytic cuff. Therefore, these nine tissues were further scored based on six categories previously described (Table 3.1.). The results are shown in Table 4.1. Images of the individual H&E stained buffalo lung tissue sections of each individual animal are included in Appendix 4. The remaining three animals had changes consistent with pneumonia associated with other causes, such as aspiration.

Tuberculous lesions were characterised by granulomatous inflammation that expanded and obscured portions of the pulmonary interstitium. Lesions ranged from focal to multifocal or multiple coalescing granulomas, with varying diameters. Granulomas contained central cores of hypereosinophilic and smudged (necrotic) debris, portions of which were deeply basophilic and granular or fragmented (mineralised). Necrotic cores were surrounded by variable numbers of epithelioid macrophages and MNGCs. Granuloma walls also contained lymphocytes. Some granulomas were bordered by concentric accumulations of hypocellular, collagen-rich, and dense fibrous tissue (fibrosis) indicative of “chronicity”. The appearance of the granulomas was noted and images of representative granulomas with different sub gross appearances shown in Figure 4.2a-c.

Of the nine buffalo lung tissues examined, lymphocytes were present in abundance in all of the granulomas. In addition, every granuloma had MNGCs present, however their numbers varied. Only one tissue section possessed granulomas that had no necrosis (buffalo 2), i.e., stage I granulomas. The rest of the granulomas in the buffalo lung tissue sections had necrosis. Only 6 of the 20 granulomas were mineralised and fibrous encapsulation was evident in all lung tissue sections except for buffalo 10.

Tuberculous lesions were scored to provide a histologic stage for the granulomatous inflammation (based on the criteria in Table 3.2.), and these results are summarised in Table 4.1. Representative images of the four stages are shown in Figure 4.3.

Table 4.1. Summary of *M. bovis* pulmonary lesion (gross and microscopic) scores as well as histologic stage for buffalo samples collected in 2018. Total score for each granuloma without tissue destruction = necrosis, mineralisation, MNGCs, lymphocytes and fibrosis.

Sample #	Gross score	Histologic diagnosis (TB or not TB)	# discrete granulomas/ sub gross appearance	Tissue destruction	Necrosis	Mineralisation	MNGCs	Lymphocytes	Fibrosis	Total score w/o (w) tissue destruction	Median score with tissue destruction	Overall histologic stage (I, II, II, IV)
1	3	Not TB			N/A							
2	3	TB	9 (one large coalescing granuloma, eight focal granulomas)	3	2	1	2	2	3	7 (10)	10	IV
					0	0	2	2	2	6 (9)		
					1	0	2	2	2	7 (10)		
					0	0	3	2	2	7 (10)		
					1	0	2	2	2	7 (10)		
					0	0	2	2	2	6 (9)		
					1	0	2	2	2	7 (10)		
					1	0	1	2	2	6 (9)		
					0	0	3	2	2	7 (10)		
3	2	Not TB			N/A							
4	1	TB	3 (two large coalescing, one focal)	3	3	1	1	3	3	11 (14)	13	IV
					3	0	1	3	3	10 (13)		
					3	0	1	3	3	10 (13)		
5	3	Not TB			N/A							
6	3	TB	0.5 (large, focal)	2	2	1	2	2	2	9 (11)	11	IV
7	1	TB	0.5 (large, focal)	2	3	1	2	1	2	9 (11)	11	IV
8	2	TB	2 (two coalescing)	2	3	1	2	3	0	9 (11)	11	IV
9	3	TB	1 (coalescing)	3	2	0	1	1	2	8 (9)	9	III
10	2	TB	1 (large, focal)	1	1	0	2	3	2	8 (9)	9	III
11	2	TB	1 (large, focal)	2	2	1	3	3	2	11 (13)	13	IV
12	3	TB	1 (coalescing)	3	2	0	1	2	3	10 (11)	11	IV

MNGCs – multinucleated giant cells; w/o – without; w – with. Text highlighted in blue indicates the data from coalescing lesions.

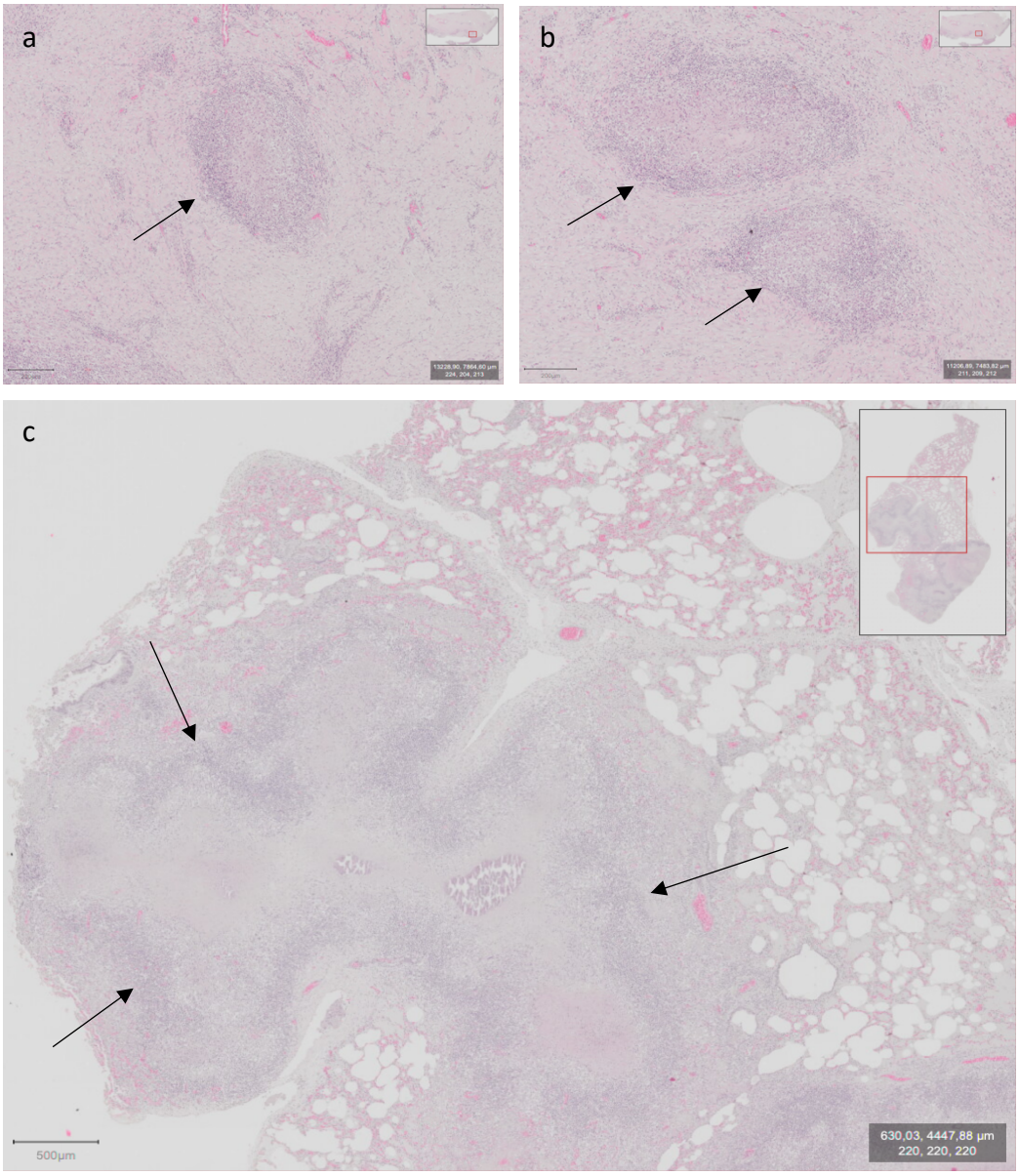

Figure 4.2. Photomicrographs of H&E stained buffalo lung tissue sections scanned at 40x magnification. Examples of tissues sections with differing sub gross appearance scores are shown: (a) arrow indicating a focal granuloma, presented at a resolution of 3.16x; (b) multiple separate granulomas (as indicated by the two arrows), presented at a resolution of 3.16x; (c) arrows pointing to the periphery of multiple coalescing granulomas, presented at a resolution of 0.45x.

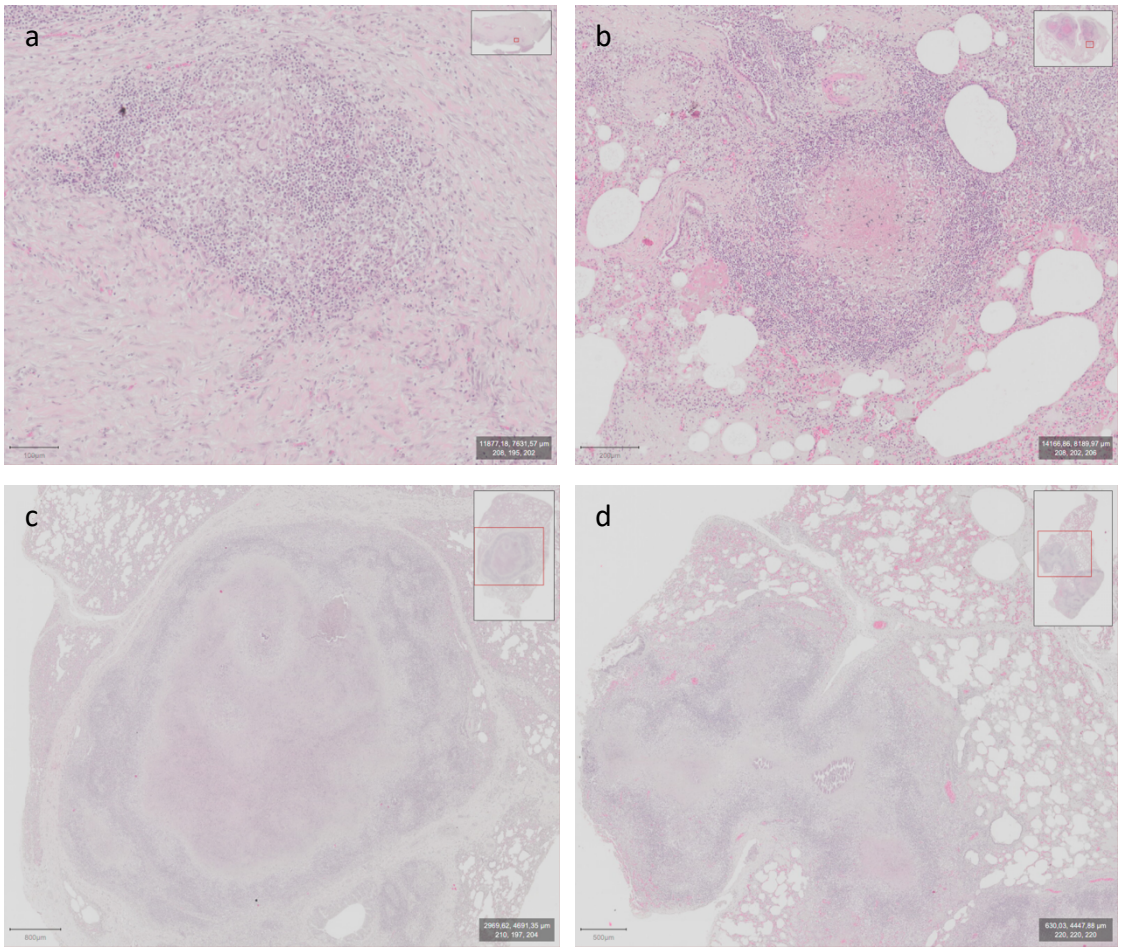

Figure 4.3. Photomicrograph of H&E-stained buffalo lung tissue sections, scanned at 40x magnification, showing; (a) a stage I granuloma in buffalo 2, presented at a resolution of 3.8x; (b) a stage II granuloma in buffalo 4, presented at a resolution of 3.8x; (c) a stage III granuloma in buffalo 13, presented at a resolution of 0.5x; (d) a stage IV granuloma in buffalo 2, presented at a resolution of 0.5x.

Out of the buffalo lung tissue sections examined, overall histologic stage III or IV were assigned to tissue sections, based on inclusion of tissue destruction score. Some tissues (e.g. buffalo 2) contained lesions that were consistent with a lower histologic stage in combination with higher histologic stage lesions, when scores did not include total tissue destruction. The majority (7 out of 9) buffalo lung tissues were assigned to stage IV, and two were assigned to stage III. Out of the four tissues with a gross score of 3, three were scored as stage IV and one as stage III; out of the three tissues with a gross score of 2, two were categorised as stage IV and one categorised as stage III; finally, both of the tissues with a gross score of 1 were categorised as staged IV granulomas.

In order to assess the presence of mycobacteria in the granulomas, buffalo lung sections were stained with ZN. However, no acid-fast bacilli were observed in any of the granulomas examined and only the blue counterstain was evident.

Immunohistochemistry

Initial optimisation with formalin-fixed buffalo lung tissues

Washington State University (WSU) monoclonal antibodies

Despite applying varying antibody dilutions, incubation times and antigen retrieval methods (Table 4.2.), no specific immunolabeling was detected for any of the WSU antibodies tested on formalin-fixed buffalo lung tissue. Only diffuse nonspecific background staining was observed (Figure 4.4).

Table 4.2. Different parameters tested, including the antibody dilution, the antigen retrieval method and the incubation time of the primary antibody, in order to optimise the immunohistochemical staining of formalin-fixed buffalo lung sections with the Washington State University antibodies to immune cell surface markers.

Antibody	Supplier	Specificity	Antibody dilution	Incubation time (min)	Antigen retrieval method
CD3	Washington State University monoclonal antibody center	Pan T cell	1/50; 1/100; 1/250; 1/500; 1/1000	30; 60	ER1; ER2
CD4		CD4 T cell			
CD8		CD8 T cell			
CD163		Macrophage			
CD335		Natural Killer cell			
MM20A		Neutrophil			

ER - epitope retrieval

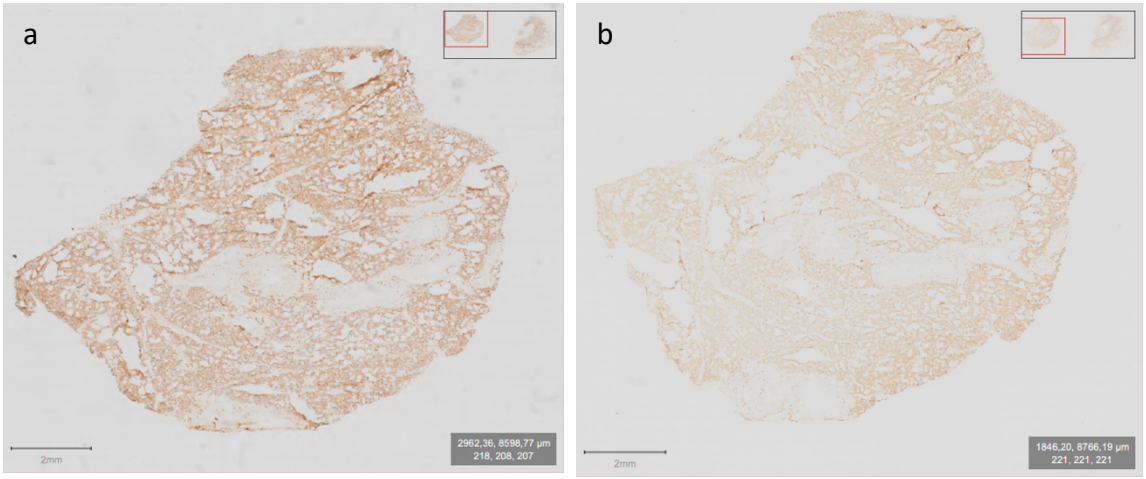

Figure 4.4. Photomicrograph scanned at 40x magnification of the CD163 WSU monoclonal antibody stained buffalo lung tissue (buffalo 3) that had been fixed in 10% buffered formalin for a year (a); (b) the negative control buffalo lung tissue (i.e. exclusion of the primary antibody); both presented at a resolution of 0.35x.

Use of beta actin antibody as a positive control for sample staining

Based on the lack of specific staining of the WSU antibodies in the formalin-fixed buffalo lung tissue, an antibody to beta actin from a different supplier, Abcam South Africa (Ab8227), was used to stain additional sections. To determine the ability of the antibodies to stain differently processed tissues, frozen and formalin-fixed cattle lung tissues were stained with antibodies to beta actin. The cattle tissue had been fixed in formalin for only 48 hours opposed to the initial buffalo tissue used, which had been fixed in formalin for more than a year. Specific staining with beta actin antibody was observed in both frozen and formalin-fixed cattle tissue (Figure 4.5).

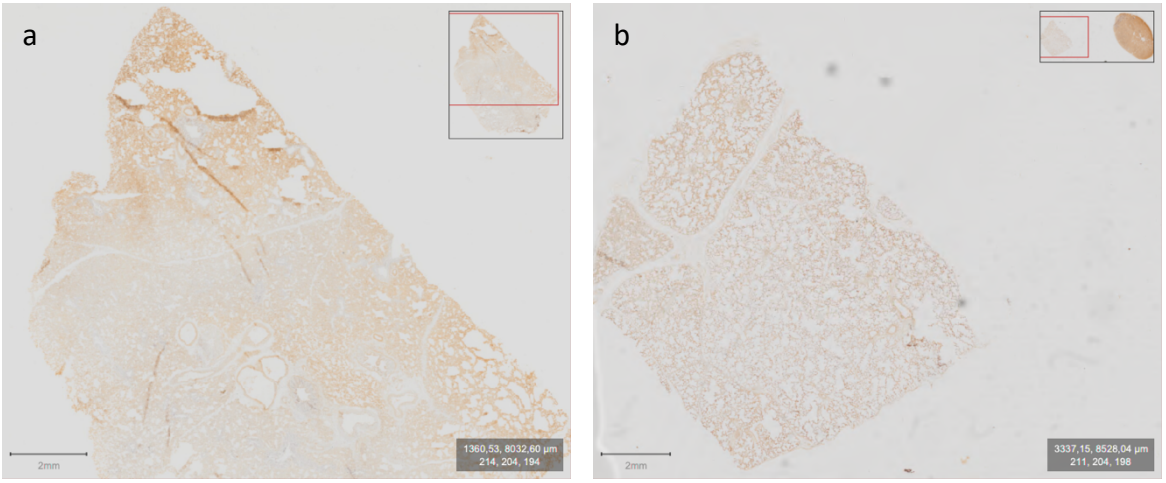

Figure 4.5. Photomicrograph scanned at 40x magnification and presented at a resolution of 0.35x, of the beta actin Abcam antibody stained cattle lung tissue that had been frozen (a) or fixed in 10% buffered formalin for 48 hours (b). Negative controls not imaged.

Beta actin was seen in abundance in the year-long formalin-fixed buffalo lung tissue (Figure 4.6a) and not in the negative control (Figure 4.6b). Since beta actin showed specific staining in both cattle and buffalo tissue, it was confirmed as a positive staining control.

Trial of WSU antibodies on frozen and formalin-fixed cattle lung tissues

Staining with the WSU CD3 antibody on frozen and formalin-fixed cattle lung tissues was performed, however, staining was only successful with the frozen but not with the formalin-fixed cattle tissue sections (images not shown). Since the WSU antibodies were not able to stain formalin-fixed tissues, a new batch of antibodies was ordered.

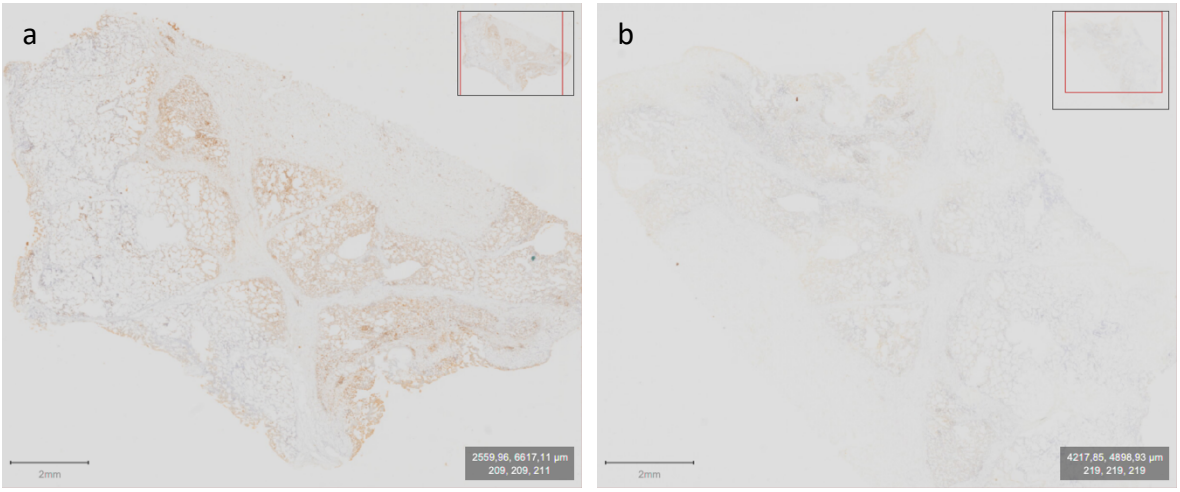

Figure 4.6. Photomicrograph scanned at 40x magnification and presented at a resolution of 0.35x, of the Abcam beta actin antibody staining of buffalo lung tissue (buffalo 1) that had been fixed in 10% buffered formalin for a year (a); (b) the negative control (i.e. exclusion of the primary antibody).

Trial of Abcam antibodies on formalin-fixed cattle and frozen then formalin-fixed buffalo lung tissues

Antibodies to cell surface markers (listed in Table 4.2) were ordered from the same supplier as the antibody to beta actin (Abcam). The Abcam antibodies were also able to stain cattle tissue that had been fixed in formalin for only 48 hours, validating their compatibility with short-term formalin-fixed tissues. The antibodies showed specific staining on frozen then formalin fixed (for 48 hours) buffalo lung tissue sections but not year-long formalin fixed buffalo tissues. Since the only available buffalo tissues were either year-long formalin-fixed or frozen then formalin-fixed, therefore, the latter were used for IHC.

A summary of results for staining of tissues stored as frozen, year-long fixation in formalin, or frozen then fixed in formalin for 48 hours, using different antibodies for IHC staining are shown in Figure 4.7**.**

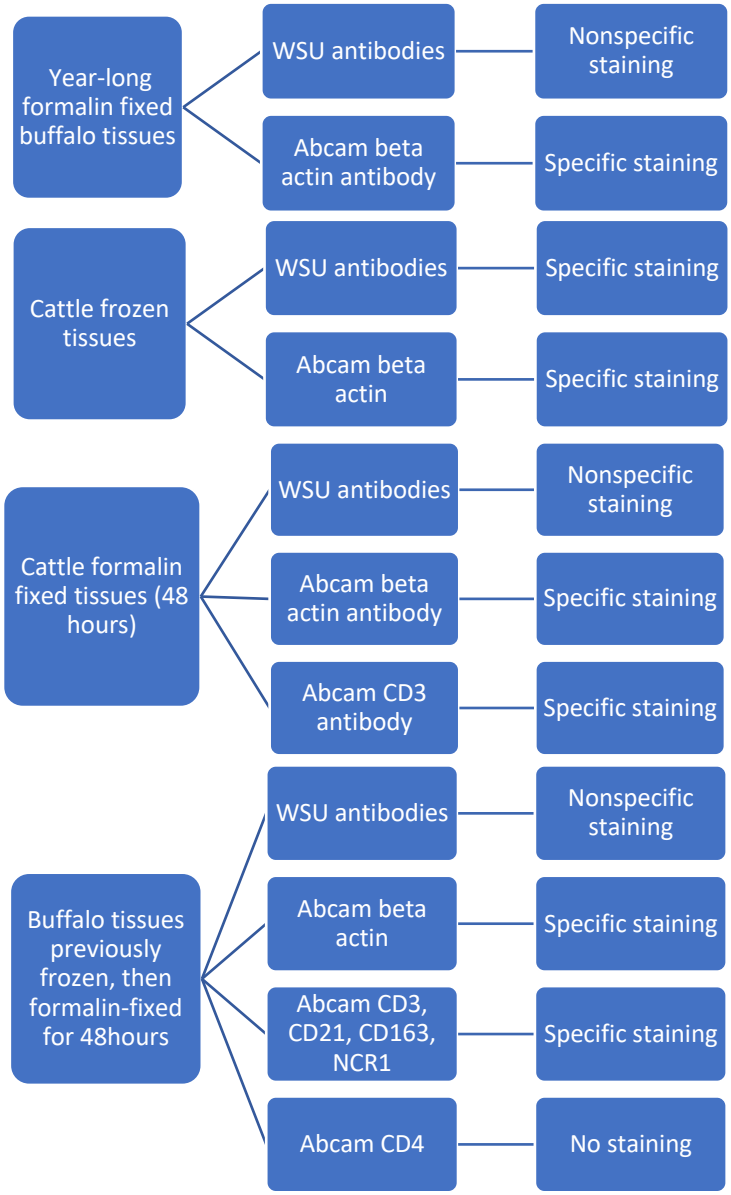

Figure 4.7. Diagram summarising the results from the optimisation process of the IHC protocol, including the lung tissues used and the antibodies tested, resulting in successful (specific) staining combinations. Combinations that did not result in successful staining either had nonspecific staining or no antibody cross-reactivity (no staining).

Staining with Abcam antibodies on frozen then formalin-fixed buffalo lung tissues

Human tissue controls

All the antibodies were first tested on human formalin-fixed tonsil tissue as a positive control (since Abcam antibodies were raised to human cell surface markers) and subsequently on formalin-fixed cattle tissue to ensure cross-species reactivity. The selected antibodies all showed specific staining on the human tonsil tissue sections (Figure 4.8). Specific staining of cells using all the Abcam antibodies to surface markers was evident in the cattle frozen lung tissue, verifying the cross-species reactivity of the antibodies to bovine immune cells (data not shown).

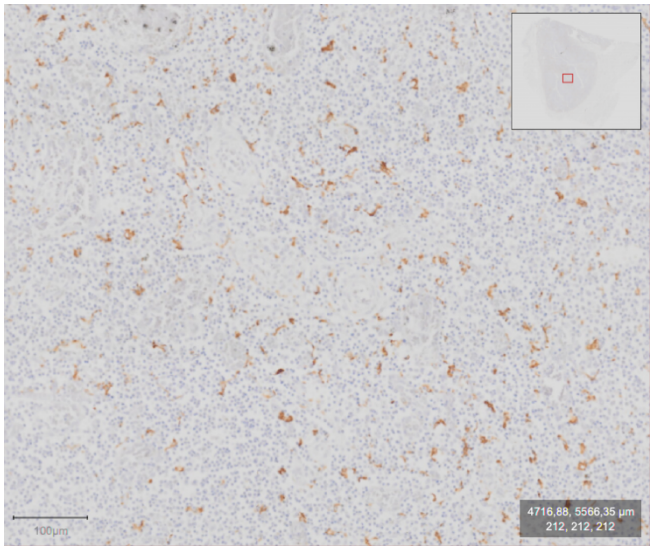

Figure 4.8. Photomicrograph, scanned at 40x magnification and presented at a resolution of 5.87x, of the CD163 Abcam antibody stained formalin-fixed human tonsil tissue.

The antibodies were used to stain frozen, then formalin-fixed buffalo lung tissue sections, and all antibodies showed immune cell specific staining, except for CD4. The details of the optimised antigen retrieval, incubation time, and dilution factor for each antibody are shown in Table 4.4. Initially tissue sections of 5 µm thickness were cut, however, subsequently sections of 1 µm thick were used as thinner sections showed reduction in the background staining observed with some of the antibodies.

Table 4.3. Summary of optimised primary antibody dilution, antigen retrieval, and incubation time for the staining of frozen-formalin-fixed buffalo lung tissue sections with Abcam antibodies to cell surface markers.

Antibody	Supplier	Specificity	Antibody dilution	Incubation time (min)	ER
CD3	Abcam South Africa	Pan T Cell	1/100	30	ER1
CD4		CD4 T Cell	NC		NC
CD21		B cell	1/250		ER2
CD163		Macrophage	1/1000		ER1
NCR1		Natural Killer Cell	1/500		ER2

NC – not compatible; ER1 – epitope retrieval 1; ER2 – epitope retrieval 2

Specific antibody staining patterns in buffalo pulmonary granulomas

Since serial sections from tissue samples used for H&E analysis were not suitable for IHC (due to long-term formalin fixation), frozen then formalin-fixed buffalo tissues were stained with Abcam cell surface marker antibodies. Therefore, since different buffalo samples were selected, it was not possible to assess histologic scores and IHC staining patterns. However, antibodies to immune cell surface markers were used to determine cell distribution in pulmonary granulomas to illustrate immune cell specific staining patterns.

CD3 (T lymphocytes)

There were CD3+ cells present in all the buffalo pulmonary granulomas examined. In tissues with a histologic appearance of a stage I or II granuloma, localised positive staining cells were seen towards the center and extending into the wall of the granulomas. In tissue sections with the histologic appearance of a stage III or IV granuloma, positive staining CD3 cells were evident towards the periphery of the granuloma (Figure 4.9a).

CD4 (T lymphocytes)

The antibody to CD4 was able to stain cells in the human tonsil control tissue (data not shown). However, there were no positively stained lymphocytes in any of the buffalo lung tissue sections that were frozen then formalin fixed. The antibody was tested at various dilutions on the buffalo tissues using both antigen retrieval methods, however, no staining was achieved,

and therefore, the distribution of this marker in buffalo pulmonary granulomas could not be assessed in this study.

CD21 (B lymphocytes)

Buffalo lung tissue sections stained with the antibody to CD21 showed a few, scattered lymphocytes, in the layer of lymphocytic infiltration in granulomas with the appearance of a histologic stage of III or IV. The positively stained lymphocytes were located peripherally to the core of granulomas and was found in clusters as shown in Figure 4.9b. Positive CD21 stained cells were not observed in granulomas with an appearance of histologic stage I or II (data not shown).

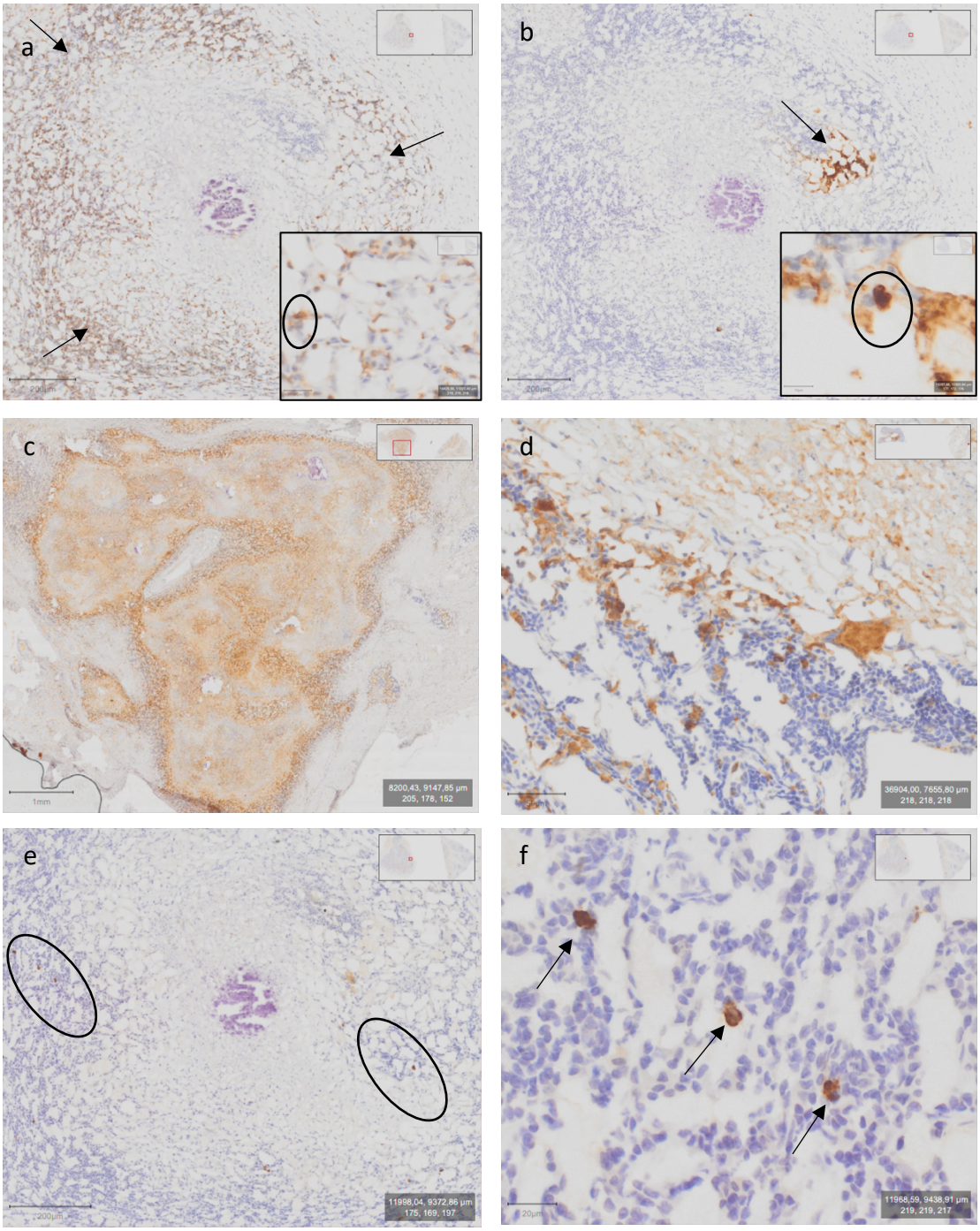

Figure 4.9. Photomicrographs scanned at 40x magnification of examples of the different antibody staining patterns observed in frozen then formalin-fixed buffalo lung tissue from buffalo 2; (a) example of the pattern of CD3+ stained cells regularly distributed around the periphery of the granuloma, as indicated by the three arrows, presented at 2x magnification, circle depicts a typical positively stained CD3+ lymphocyte, presented at a resolution of 34.93x; (b) example of CD21 antibody stained cells in buffalo lung tissue, showing the clusters of positive cells in the areas of lymphocytic infiltration of the pulmonary granuloma, presented

at a resolution of 2x, the circle depicts a typical positively stained CD21 cell, presented at a resolution of 75.63x; (c) example of CD163 antibody stained cells in buffalo lung granuloma, presented at 0.5x; (d) example of an individual CD163 stained cell, indicated by the arrow, presented at a resolution of 5x; (e) example of NCR1 antibody stained cells in buffalo lung granuloma, showing single scarce scattered cells around the periphery of the granuloma (circles), presented at a resolution of 2x; (f) example of individual NCR1 stained cells, indicated by the arrows, presented at a resolution of 8x.

CD163 (macrophages)

Staining with the antibody to CD163 showed positive stained cells in all granulomas examined in this study. Some non-specific staining was apparent (Figure 4.9c) but could be differentiated from cell staining at higher magnification (Figure 4.9d). CD163 positively stained cells were scattered randomly in stage I and II granulomas and located peripherally to the necrotic center of stage III and IV granulomas. CD163 stained both macrophages as well as MNGCs (Figure 4.9d).

NRC1 (natural killer cell)

Staining of buffalo lung tissue sections with the NCR1 antibody revealed scarce single positively stained cells scattered randomly in granulomas. These cells were not seen in abundance in any stage of granuloma. As necrotic areas of granulomas increased in size, NK cells appeared to be pushed to the periphery of granulomas (Figure 4.9e and f).

Chapter 5: Discussion

To understand host immune responses towards *M. bovis* infection, this study describes the gross and histopathological characteristics of pulmonary granulomas in a group of naturally infected *M. bovis* culture-positive African buffaloes (*Syncerus caffer*). In addition, an immunohistochemical method for African buffalo lung tissue was optimised to identify and evaluate the distribution of selected immunological cell markers in granulomas.

Histopathologic sample analyses

In this study, histologic lesion scores were compared with gross lesion scores determined at the time of necropsy, as per Palmer *et al*. (2007). Gross lesion scores, based on the guidance of previously published work (Palmer *et al*., 2007), did not always appear to correlate with histologic lesions. This was evident: 1) in cases of bTB in which gross lesions were low scoring or were missed, but in which more extensive histologic changes were present, (i.e., both samples with an assigned gross lesion score of 1 had multiple coalescing granulomas microscopically); and 2) cases in which the gross score mischaracterised gross lesions as bTB when they were due to non-TB pneumonia. These findings reiterate that gross assessment alone is unreliable for diagnosing bTB and determining the extent and severity of disease in buffalo lungs.

Study findings also included descriptions of microscopic lesion morphology in cases of *M. bovis* pulmonary infection in buffalo. Analyses revealed that some characteristics of bTB granulomas in buffaloes were similar to those described in cattle (Palmer *et al.,* 2016). The high number of macrophages observed in buffalo pulmonary granulomas was similar to what has been observed in early granuloma stages in species such as fallow deer and wild boar (Garćia-Jiménez *et al.,* 2012, 2013). Buffalo granulomas contained epithelioid macrophages and MNGCs. These cells are characteristic of early stages of granuloma development (McClean and Tobin, 2016). Epithelioid macrophages respond to inflammatory stimuli, and are highly phagocytic (Ramakrishnan, 2012). The MNGCs were distinctive in the H&E stained lung sections and were characterised as histiocytic cells containing multiple nuclei generally arranged in a horseshoe pattern (Langhans' type giant cells). The relative abundance and distribution of lymphocytes in buffalo lung granulomas were similar to bTB granulomas described in other species and may indicate similar pathogenesis. Granulomas in fallow deer have a high percentage of lymphocytes, also observed in buffalo lung granulomas (Garćia-Jiménez *et al.,* 2012). This is suggestive that the initial immune responses in buffalo,

like fallow deer and cattle, are likely to be mediated by the combined actions of lymphocytes and macrophages. Although lymphocyte infiltration was substantial in the majority of granulomas examined, a distinctive peripheral "cuff" of lymphocytes around the core was observed in granulomas with necrosis.

Larger, more extensive foci of granulomatous inflammation tended to be associated with a larger area of central necrosis. Findings suggested necrosis was a feature of more advanced or chronic lesions. In buffalo pulmonary granulomas, central necrosis was surrounded by macrophages interspersed among the lymphocytic infiltrate, similar to those seen in badgers (Gormley and Corner, 2018). Buffalo bTB granulomas, similar to observations in cattle, appear to develop necrosis (Domingo *et al.,* 2014). Some granulomas were surrounded by rims of fibrosis which was indicative of chronicity. Studies have shown that fibrotic granulomas are associated with a high bacterial burden (Warsinske *et al.,* 2017). The connective tissue capsule is formed by fibroblast cells in response to TGF-β, IL-13, structurally and functionally related pro-inflammatory cytokines, and the anti-inflammatory cytokine IL-4, which is released by epithelioid macrophages (Domingo *et al.,* 2014; Pagán and Ramakrishnan, 2018).

In many of the buffalo lung sections examined, coalescing lesions took up the majority of the slides. In these sections, very little to no normal-looking lung architecture was present. However, these lesions contained less mineralisation than described in advanced cattle granulomas (Wangoo *et al.,* 2005). Therefore, an adjustment to the current cattle granuloma scoring criteria would be needed to fit what has been observed in buffalo granulomas. A spectrum of morphologic changes, including some features compatible with a more acute course and those indicative of chronicity, were not evident. In order to understand the development of bTB lesions in buffalo, it is useful to classify buffalo granulomas as low- or high-stage granulomas based on their morphology. Using observations from this study, a stage I or II bTB granuloma in buffalo lung has scattered MNGCs at the core, surrounded by lymphocytes, and lacking features such as necrosis and mineralisation, and may or may not have a thin fibrous capsule. A high-stage (III or IV) granuloma would contain a necrotic core that could be focal or comprised of multiple coalescing lesions and may or may not contain mineralisation, surrounded by a lymphocytic cuff, and a thick fibrous capsule. Based on the limited samples in this study, it appears that mineralisation is not a defining feature of a high-stage granuloma in buffalo lung tissue.

The presence of acid-fast bacilli in the core of the granuloma provides evidence to support an association between the granuloma and mycobacterial infection (Carrisoza-Urbina *et al.,* 2019). However, in this sample set, ZN staining revealed no bacilli in any of the *M. bovis* culture-positive buffalo lung samples. One explanation is that *M. bovis* infection in buffaloes may be paucibacillary, i.e., infection with few or no detectable bacilli present in lesions. In a study performed in elephants, the negative ZN staining result included the presumption of paucibacillary infection with mycobacteria, amongst other factors (Feldman *et al.,* 2013). This finding could indicate that a low bacterial burden is sufficient in eliciting an immune response in buffaloes, however more cases to investigate the prevalence of paucibacillary infections in buffalo should be looked into. An alternate method for detection of bacilli could be to use a pan-TB IHC stain in which antibodies towards mycobacterial antigens on the surface of the cells could be detected (Goel and Budhwar, 2007). Another alternate method for the detection of *M. bovis* would be to test for *M. bovis* nucleic acids using in situ hybridization (Fenhalls *et al.,* 2002). Fluorescent in situ hybridisation (FISH) uses fluorescent labelled probes to hybridise specifically to complementary target sequences within a cell (Yuan *et al.,* 2015). A second reason for the unsuccessful ZN stains could be due to the fact that only one section was taken from each granuloma. A granuloma is a three-dimensional structure and multiple sections from the same lesion might have revealed the presence of acid-fast bacilli.

IHC optimisation

IHC was optimised to establish a staining technique for buffalo tissues to determine the distribution of immune cell populations. Initial assays were unsuccessful with diffuse nonspecific staining and lack of antigen target labeling, most likely due to prolonged formalin fixation of tissue. Formalin is a cross-linking fixative, and extended immersion time results in bonds throughout tissues that hinder antigen retrieval for downstream assays like IHC (Kabiraj *et al.,* 2015). Because buffalo samples had remained in formalin for greater than one year prior to analyses, absence of specific labeling in the tissues, following staining with the initial set of antibodies (WSU), was presumed to be a consequence of prolonged formalin fixation. This presumption was supported by successful staining of cattle frozen tissue sections using the WSU CD3 antibody. However, buffalo frozen tissue samples, that had been thawed then fixed in formalin for 48 hours and stained with the WSU antibodies, showed no staining. These results suggested a lack of antibody cross-reactivity with the buffalo tissues. Given the challenges of these initial optimisation experiments, protocol modifications and additions were adopted. To control for variable steps in the immunohistochemical staining protocol, samples

of cattle and buffalo tissues were first stained with antibodies against beta actin. Beta actin is a highly conserved protein that is involved in cell motility, structure, and integrity in mammalian tissues and immunolabeling indicated successful target epitope retrieval (NCBI, 2020). To address the issue of lack of antibody cross-reactivity, antibodies from another source were identified and evaluated for their ability to successfully stain cattle and buffalo tissues.

IHC sample evaluation

As previously observed in the H&E stained buffalo lung tissues, early granulomas showed a preponderance of macrophages. The CD163 cell marker was able to stain both epithelioid macrophages and MNGCs. Epithelioid macrophages and MNGCs formed the core of the granuloma in lower histologic stage granulomas, but with lesion progression, macrophages were peripherally located to the necrotic core. MNGCs are known to produce specific cytokines and chemokines, namely TNF-α, IFN-γ, and IL-12, which play roles in the initial stages of granuloma formation (Cavalcanti *et al,* 2012). These are critical pro-inflammatory cytokines that stimulate migration of immune cells to the site of infection, facilitate activation of macrophages, and mediate the production of reactive nitrogen intermediates, which enhance the bactericidal function of macrophages (Cavalcanti *et al.,* 2012).

In this study, T lymphocytes were seen in abundance in all bTB granulomas, regardless of differing appearance associated with histologic stages, based on staining with the antibody to CD3. However, staining of buffalo lung (frozen then formalin-fixed) tissues with the selected CD4 antibody was unsuccessful, preventing further characterisation of T lymphocyte subpopulations. In the study done on cattle samples by Palmer *et al.* (2007), the cattle samples were incubated with the CD4 antibody overnight. This could be a reason for the CD4 antibody not working on the buffalo samples in this research as the samples were not incubated with CD4 overnight. In studies of *M. tuberculosis* in lung granulomas of mice and humans, CD4+ cells were widely distributed, also comprising the majority of the lymphocytic infiltration (Gonzalez-Juarrero, 2001). In cattle, CD4+ cells were the predominant T cell subset present in tuberculoid pulmonary granulomas (Palmer *et al.,* 2007). CD4+ cells are known to be central to immunity against mycobacterial infections and a source of IFN-γ, which stimulates activation of macrophages (Cavalcanti *et al.,* 2012; Palmer *et al.,* 2019). Although antibodies to CD8 were not evaluated in this study, in humans with *M. tuberculosis* infection, CD8+ T cells were shown to also produce IFN-γ and TNF-α (El Fenniri *et al.,* 2011). In cattle

granulomas, CD8+ T cells were less numerous than CD4+ cells and localized to granuloma margins (Wangoo *et al.,* 2005).

In buffalo granulomas with characteristics of a high histologic stage, CD3+ cells were found primarily in the granuloma wall. The same observation was reported in *M. bovis* granulomas in cattle by Wangoo *et al* (2005). B cells (CD21+) were not as abundant in the buffalo granulomas as T cells, only making up a small proportion of total lymphocytes, based on subjective assessment. Though B cells have been reported in early cattle granulomas, B cells were not seen in buffalo granulomas with analogous morphology (Wangoo *et al.,* 2005). In buffalo granulomas with the appearance of a high histologic stage, B cell clusters were scattered in the lymphocytic cuff. There was a general trend of increasing CD21+ cell numbers as the lesions became more advanced and noticeable clusters of B cells have been documented in advanced granulomas in cattle and humans (Aranday-Cortes *et al.,* 2013; Ulrichs *et al.,* 2004). It has been suggested that these clusters contain antigen-presenting cells and B cells at different stages of differentiation, surrounded by CD4+ and CD8+ lymphocytes (Salguero *et al.,* 2016). The combination of B cells and CD4+ and CD8+ T lymphocytes is considered vital in directing a coordinated host response to mycobacteria (Salguero *et al.,* 2016).

Scattered single NK cells occurred in similar numbers in buffalo lung granulomas that appeared to have differing histologic characteristics (stages), based on staining with the antibody to NCR1. However, they did not make up a major component of the cellular population in buffalo lung granulomas, suggesting a minimal role in the localized immune response and bTB pathogenesis.

Limitations

There were a number of limitations in this project that impacted interpretation of the results. First, the limited sample availability influenced study power. The small sample size precluded statistical analyses to identify differences in immune cell types and numbers between buffalo granulomas of varying gross and histologic lesion scores. For example, there were only two samples with a gross lesion score of 1 and when examined microscopically, both these slides showed granulomas with a high histologic stage. If a larger sample set was available, correlation, or lack thereof, between gross and histologic lesion scores may have been more evident. Another limitation was that only a single sample from each animal was evaluated.

Multiple samples from the lung of the same buffalo would have allowed for a more comprehensive overview of pathologic changes occurring in that animal. In addition to sample size, sample fixation was another obstacle in this project. Because original buffalo samples collected in the field were stored in formalin for a prolonged period, these samples were not appropriate for IHC analyses. Frozen tissues were available and used after thawing and fixation in formalin for 48 hours for IHC; however, this prevented immunolabeling from being performed on serial sections of the same lesions that had been evaluated for histologic scoring. Consequently, it was not feasible to directly correlate IHC results with lesions described in the H&E stained sections. Ideally, samples should be fixed in formalin for a short period then embedded, which would allow serial sections to be stained with H&E and antibodies for IHC in the same tissue. A limitation of the staging system used in this project was that the overall score given to a tissue sample, as well as individual granulomas, based on the stated criteria, did not always reflect what was seen under the microscope. For example, a granuloma could have many MNGCs (score 3), a large lymphocytic infiltration (score 3) and be categorised as a stage II granuloma, however, under the microscope it is evident that this is only a stage I granuloma. Therefore, further refinement of these criteria is needed. This could be done by weighting the scores differently.

Other limitations included the failure of detection of acid-fast bacilli in sections to confirm the presence of *M. bovis* bacilli. The inability to confirm duration of infection to correlate gross and histologic scores with disease progression since the study used free-ranging buffaloes naturally infected with *M. bovis*; and the absence of other data on the health of study animals that may have influenced overall immune responses and development of pulmonary bTB granulomas.

Finally, analyses of T lymphocyte subsets could not be performed since the CD4 antibody did not stain buffalo lung tissue, possibly owing to the lack of cross-reactivity of this antibody with bovine cell surface markers, as the antibodies were generated to human cell surface markers. Additionally, the supplier of the antibodies used in this study did not have a CD8 antibody known to cross-react with bovine tissues. Therefore, the single set of antibodies screened for IHC staining of buffalo lung sections limited the ability to detect all the key immune cell populations.

Chapter 6: Conclusion

African buffaloes (*Syncerus caffer*) are recognised wildlife maintenance hosts for *M. bovis* in South Africa. There are significant knowledge gaps regarding differences in bTB pathogenesis among affected species. By investigating pathological changes, insights into local host responses can provide valuable information to bridge such knowledge gaps. Understanding of the comparative pathogenesis and immunology of bTB in different species is essential to diagnosing infection and disease, as well as informing animal management strategies. In order to better understand the pathogenesis of bTB in African buffaloes, this study was performed using animals naturally infected with *M. bovis.* The primary aim was the characterisation of immune cell populations present in buffalo lung samples with different macroscopic changes and was achieved by visual examination of H&E stained tissue sections to assess the microscopic appearance of the granulomas. Defining and understanding lesion morphology can provide insight into disease progression.

Mycobacterial granulomas are dynamic, with cell populations that actively change during the course of infection. The microscopic features of bTB granulomas in buffalo lung tissue were described in this study and used to stage the granulomas. The appearance of granulomas in African buffaloes closely resembled those seen in cattle. However, the buffalo granulomas with advanced histologic stage contained less mineralisation, than reported in cattle granulomas at the same stage. Therefore, the granuloma classification suggested in this study was adjusted by modifying the criteria used in cattle and provides a description that will facilitate further studies on bTB granuloma development in African buffaloes. In addition, an immunohistochemistry protocol was optimised for buffalo lung tissues, except for CD4, and contributed to the identification of selected immune cell populations involved in granulomas. This study highlights the necessity for a species-specific granuloma scoring criteria for African buffaloes. Although only a small sample size was available, the results of this study contribute toward i) a basis for the further development of buffalo specific granuloma classification criteria; ii) a more comprehensive characterisation of local host responses to mycobacterial infection in buffaloes, which, in turn, can provide insight for correlates of infection status; and iii) provide information for development of diagnostic biomarkers for bTB in African buffaloes.

Future directions

Future research using a larger sample size is recommended to confirm the findings of this study. The route of transmission may determine the location and spectrum of lesions observed in bTB (Domingo *et al.,* 2014). Inhalation is the most common route of infection and causes lesions in the thoracic lymph nodes and lower respiratory tract (Domingo *et al.,* 2014). It would, therefore, be beneficial to include lymph node samples in addition to lung samples in these studies to assess the immune responses in various tissues. Further studies should also ensure the inclusion of buffalo samples that have been in fixed formalin for 24-48 hours which will preserve cellular morphology and facilitate matched histopathologic and immunohistochemical analysis. These studies would enable a more comprehensive description of buffalo immune responses to *M. bovis* and investigate associations between the H&E and IHC results, as well as comparing these to systemic immune responses based on cytokine assays. Lastly, future studies would also benefit from additional panels of antibodies for IHC staining of buffalo tissue sections. Other methods to assess local immunity, in addition to IHC, could include in situ hybridisation to investigate the precise localisation of specific immune mediators within cells in the granuloma.

References

Álvarez, Á., Estrada-Chávez, C. and Flores-Valdez, M. (2009). Molecular findings and approaches spotlighting *Mycobacterium bovis* persistence in cattle. *Veterinary Research*, 40(3): 22.

Anderson, J. M., Rodriguez, A. and Chang, D. T. (2008). Foreign body reaction to biomaterials. *Seminars in Immunology,* 20(2): 86-100.

Ayele, W. Y., Neill, S. D., Zinsstag, J., Weiss, M. G. and Pavlik, I. (2004). Bovine tuberculosis: an old disease but a new threat to Africa. *International Journal of Tuberculosis Lung Disease*, 8(8): 924-937.

Bailey, S. S., Crawshaw, T. R., Smith, N. H. and Palgrave, C. J. (2013). *Mycobacterium bovis* infection in domestic pigs in Great Britain. *The Veterinary Journal,* 198: 391-397. https://doi.org/10.1016/j.tvjl.2013.08.035

Bernitz, N., Goosen, W. J., Clarke, C., Kerr, T. J., Higgitt, R. *et al.* (2018). Parallel testing increases detection of *Mycobacterium bovis*-infected African buffaloes (*Syncerus caffer*). *Veterinary Immunology and Immunopathology,* 204(2018): 40-43.

Bold, T. and Ernst, J. (2009). Who benefits from granulomas, mycobacteria or host? *Cell*, 136(1): 17-19.

Brites, P. and Gagneux, S. (2017). The nature and evolution of genomic diversity in the *Mycobacterium tuberculosis* complex. *Advances in Experimental Medicine and Biology,* 1019(1): 1-26.

Carow, B., Hauling, T., Qian, X., Kramnik, I., Nilsson, M. and Rottenberg, M. (2019). Spatial and temporal localization of immune transcripts defines hallmarks and diversity in the tuberculosis granuloma. *Nature Communications*, 10(1823): 1-15.

Carrisoza-Urbina, J., Morales-Salinas, E., Bedolla-Alva., Hernández-Pando, R. and Gutiérrez-Pabello, J. A. (2019). Atypical granuloma formation in *Mycobacterium bovis*-infected calves. *PLoS ONE,* 14(7): 1-17.

Carstensen, M. and Don Carlos, M. W. (2011). Preventing the establishment of a wildlife disease reservoir: a case study of bovine tuberculosis in wild deer in Minnesota, USA. *Veterinary Medicine International,* 2011(2): 413240.

Cavalcanti, Y., Brelaz, M., Lemoine Neves, J., Ferraz, J. and Pereira, V. (2019). Role of TNF-alpha, IFN-gamma, and IL-10 in the development of pulmonary tuberculosis. *Pulmonary Medicine,* 2012(745483): 1-10.

Cdc.gov. (2019). *Fact Sheets | General | Mycobacterium bovis (Bovine Tuberculosis) in Humans | TB | CDC*. [online] Available at:

https://www.cdc.gov/tb/publications/factsheets/general/mbovis.htm [Accessed 14 Aug. 2019].

Clay, H., Volkman, H. E. and Ramakrishnan, L. (2008). Tumor necrosis factor signalling mediates resistance to mycobacteria by inhibiting bacterial growth and macrophage death. *Immunity,* 29(2): 283-294.

Cooper, A. M. (2009). Cell-mediated immune responses in tuberculosis. *Annual Review of Immunology*, 27: 393-422. https://doi.org/10.1146/annurev.immunol.021908.132703

Cooper, A. M., Magram, J., Ferrant, J. and Orme, I. M. (1997). Interleukin 12 (IL-12) is crucial to the development of protective immunity in mice intravenously infected with *Mycobacterium tuberculosis. Journal of Experimental Medicine,* 186(1): 39-45.

de la Barrera, S., Aleman, M., Musella, R., Schierloh, P., Pasquinelli, V. *et al.* (2004). IL-10 down-regulates costimulatory molecules on *Mycobacterium tuberculosis*-pulsed macrophages and impairs the lytic activity of CD4 and CD8 CTL in tuberculosis patients. *Clinical Experimental Immunology,* 138(1): 128-138.

Denis, M., Keen, D. L., Parlane, N. A., Storset, A. K. and Buddle, B. M. (2007). Bovine natural killer cells restrict the replication of *Mycobacterium bovis* in bovine macrophages and enhance IL-12 release by infected macrophages. *Tuberculosis,* 87(1): 53-62.

De Vos, D., Bengis, R. G., Kriek, N. P. J., Michel, A., Keet, D.F. *et al* (2001). The epidemiology of tuberculosis in free-ranging African buffalo (*Syncerus caffer*) in the Kruger National Park, South Africa. *Onderstepoort Journal of Veterinary Research*, 68(2): 119-130

Di Paolo, N. and Shayakhmetov, D. (2016). Interleukin 1α and the inflammatory process. *Nature Immunology*, 17(8): 906-913.

Domingo, M., Vidal, E. and Marco, A. (2014). Pathology of bovine tuberculosis. *Research in Veterinary Science*, 97: 20-29. https://doi.org/10.1016/j.rvsc.2014.03.017

Drain, P., Bajema, K., Dowdy, D., Dheda, K., Naidoo, K. *et al.* (2018). Incipient and subclinical tuberculosis: a clinical review of early stages and progression of infection. *Clinical Microbiology Reviews*, 31(4): e00021-18.

Duraiyan, J., Govindaranjan, R., Kaliyappan, K. Palanisamy, M. (2012). Applications of immunohistochemistry. *Journal of Pharmacy and Bioallied Sciences*, 4(2): 307-309.

Egen, J., Rothfuchs, A., Feng, C., Winter, N., Sher, A. and Germain, R. (2008). Macrophage and T cell dynamics during the development and disintegration of mycobacterial granulomas. *Immunity*, 28(2): 271-284.

Ehlers, S. (2012). The granuloma in tuberculosis: dynamics of a host-pathogen collusion. *Frontiers in Immunology,* 3(411): 1-9.

El Fenniri, L., Toossi, Z., Aung, H., El Iraki, G., Bourkkadi, J., Benamor, J. *et al.* (2011). Polyfunctional *Mycobacterium tuberculosis*-specific effector memory $CD4^+$ T cells at sites of pleural TB. *Tuberculosis,* 91(3): 224–230.

Esin, S. and Batini, G. (2015). Natural killer cells: a coherent model for their functional role in *Mycobacterium tuberculosis* infection. *Journal of Innate Immunity,* 2015(7): 11-24.

Feldman, M., Isaza, R., Prins, C. and Hernandez, J. (2013). Point prevalence and incidence of *Mycobacterium tuberculosis* complex in captive elephants in the United States. *Veterinary Quarterly,* 33(1): 28-32.

Fenhalls, G., Stevens-Muller, L., Warren, R., Carroll, N., Bezuidenhout, J. *et al.* (2002). Localisation of mycobacterial DNA and mRNA in human tuberculous granulomas. *Journal of Microbiological Methods,* 51(2): 197-208.

Ferguson, J. S., Martin, J. L., Azad, A. K., McCarthy, T. R., Kang, P.B. *et al.* (2006). Surfactant protein D increases fusion of *Mycobacterium tuberculosis* containing phagosomes with lysosomes in human macrophages. *Infection and Immunity,* 74(12): 7005-7009.

Fischer, A. H., Jacobson, K. A., Rose, K. and Zeller, R. (2006). Haematoxylin and eosin staining of tissue and cell sections, Chapter 4. *Preparation of cells and Tissues for Fluorescence Microscopy.* Cold Spring Harbor Laboratory Press, Cold Spring Harbor, NY, USA.

Fitzgerald, S. and Kaneene, J. (2012). Wildlife reservoirs of bovine tuberculosis worldwide: hosts, pathology, surveillance, and control. *Veterinary Pathology*, 50(3): 488-499.

Fremond, C. M., Togbe, D., Doz, E., Rose, S., Vasseur., V. *et al.* (2007). IL-1 receptor-mediated signal is an essential component of MyD88-dependent innate response to *Mycobacterium tuberculosis* infection. *Journal of Immunology,* 179(2): 1178-1189.

Ganchua, S. K. C, Cadena, A. M., Maiello, P., Gideon, H. P., Myers, A. J, *et al*. (2018). Lymph nodes are sites of prolonged bacterial persistence during *Mycobacterium tuberculosis* infection in macaques. *PLOS Pathogens*, 14(11): 1-28.

Garćía-Jiménez, W. L., Fernández-Llario, P., Gómez, L., Beńitez-Medina, J. M., García-Sánchez, A. *et al.* (2012). Histological and immunohistochemical characterisation of *Mycobacterium bovis* induced granulomas in naturally infected Fallow deer (*Dama dama*). *Veterinary Immunology and Immunopathology,* 149(1-2): 66-75.

Garćía-Jiménez, W. L., Beńitez-Medina, J. M., Fernández-Llario, P., Abecia, J. A., García-Sánchez, A. *et al.* (2013). Comparative pathology of the natural infections by *Mycobacterium bovis* and by *Mycobacterium caprae* in wild boar (*Sus scrofa*). *Transboundary and Emerging Diseases,* 60(2): 102-109.

Garand, M., Goodier, M., Owolabi, O., Donkor, S., Kampmann, B. and Sutherland, J. S. (2018). Functional and phenotypic changes of natural killer cells in whole blood during *Mycobacterium tuberculosis* infection and disease. *Frontiers in Immunology,* 9(257): 1-18.

Goel, M. M. and Budhwar, P. (2007). Immunohistochemical localization of mycobacterium tuberculosis complex antigen with antibody to 38 kDa antigen versus Ziehl Neelsen staining in tissue granulomas extrapulmonary tuberculosis. *Indian Journal of Tuberculosis,* 54(1): 24-29.

Good, M. and Duignan, A. (2011). Perspectives on the history of bovine TB and the role of tuberculin in bovine TB eradication. *Veterinary Medicine International,* 2011(410470): 1-11.

Goosen, W. J., Miller, M. A., Chegou, N. N., Cooper, D., Warren, R. M. *et al.* (2014). Agreement between assays of cell-mediated immunity utilizing *Mycobacterium bovis*-specific antigens for the diagnosis of tuberculosis in African buffaloes (*Syncerus caffer*). *Veterinary Immunology and Immunopathology,* 160(2014): 133-138.

Gormley, E. and Corner, L. (2018). Pathogenesis of *Mycobacterium bovis* infection: the badger model as a paradigm for understanding tuberculosis in animals. *Frontiers in Veterinary Science*, 4: 247. https://doi.org/10.3389/fvets.2017.00247

Gunn-Moore, D. A. (2014). Feline mycobacterial infections. *Veterinary Journal,* 201(2014): 230-238.

Heemskerk, D., Caws, M., Marais, B. and Farrar, J. (2019). *Clinical Manifestations*. [online] Ncbi.nlm.nih.gov. Available at: https://www.ncbi.nlm.nih.gov/books/NBK344404/ [Accessed 1 Aug. 2019].

Helman, R. G., Russell, W. C., Jenny, A., Miller, J. and Payeur, J. (1998). Diagnosis of tuberculosis in two snow leopards using polymerase chain reaction. *Journal of Veterinary Diagnostic Investigation,* 10(1): 89-92.

Hewitt,S. M., Baskin, D. G., Frevert, C. W., Stahl, W. L. and Rosa-Molinar, E. (2014). Controls for immunohistochemistry. The histochemical society's standards of practice for validation of immunohistochemical assays. *Journal of Histochemistry and Cytochemistry,* 62(10): 693-697.

Hilleman, D., Warren, R., Kubica, T., Rüsch-Gerdes, S. and Niemann, S. (2006). Rapid detection of *Mycobacterium tuberculosis* Beijing genotype strains by Real-Time PCR. *Journal of Clinical Microbiology,* 44(2): 302-306.

Hofman, F. (2002). Immunohistochemistry. *Current Protocols in Immunology,* 49(1): 1-21.

Janeway, C.A., J., Travers, P., Walport, M. and Shlomchik, M. (2019). *Principles of Innate and Adaptive Immunity*. [online] Ncbi.nlm.nih.gov. Available at: https://www.ncbi.nlm.nih.gov/books/NBK27090/ [Accessed 27 Apr. 2019].

Jimbo, S., Suleman, M. and Maina, T. (2017). Effects of *Mycoplasma bovis* on bovine neutrophils. *Veterinary Immunology and Immunopathology,* 2017(188): 27-33.

Johnson, L., Liebana, E., Nunez, A., Spencer, Y., Clifton-Hadley, R., Jahans, K., Ward, A., Barlow, A. and Delahay, R. (2008). Histological observations of bovine tuberculosis in lung and lymph node tissues from British deer. *The Veterinary Journal*, 175(3): 409-412.

Junqueira-Kipnis, A. P., Kipnis, A., Jamieson, A. Juarrero, M.G., Diefenbach, A. *et al.* (2003). NK cells respond to pulmonary infection with *Mycobacterium tuberculosis*, but play a minimal role in protection. *The Journal of Immunology*, 171(11): 6039-6045.

Kabiraj, A., Gupta, J., Khaitan, T. and Bhattacharya, P. T. (2015). Principle and techniques of immunohistochemistry – a review. *International Journal of Biological and Medical Research,* 6(3): 5204-5210.

Keane, J., Gershon, S., Wise, R. P., Mirabile-Levens, E., Kasznica, J., Schwieterman, W. D. *et al.* (2001). Tuberculosis associated with infliximab, a tumor necrosis factor alpha-neutralizing agent. *The New England Journal of Medicine,* 345(15): 1098-1104.

Kennedy, H. E., Welsh, M. D., Bryson, D. G., Cassidy, J. P., Forster, F. I. *et al.* (2002). Modulation of immune responses to *Mycobacterium bovis* in cattle depleted of $WC1^{+}$ cells. *Infection and Immunity,* 70(3): 1488-1500.

Khatri, B., Coad, M., Clifford, D., Hewinson, R., Whelan, A. and Vordermeier, H. (2019). A natural-transmission model of bovine tuberculosis provides novel disease insights. *Veterinary Record,* 171(18): 1-2.

Kim, S-W., Roh, J. and Park, C-S. (2016). Immunohistochemistry for pathologists: protocols, pitfalls and tips. *Journal of Pathology and Translational Medicine,* 50(2016): 411-418.

Laisse, C., Gavier-Widén, D., Ramis, G., Bila, C., Machado, A., Quereda, J., Ågren, E. and van Helden, P. (2015). Characterization of tuberculous lesions in naturally infected African buffalo (*Syncerus caffer*). *Journal of Veterinary Diagnostic Investigation*, 23(5): 1022-1027.

Lopez, A. and Martinson, S. A. 2017. Chapter 9. Respiratory System, Mediastinum and Pleurae. In: Zachary J. F. (ed) Pathological Basis of Veterinary Disease. 6thedition. Elsevier, St. Louis.

Lyadova, I. V. (2017). Neutrophils in tuberculosis: heterogeneity shapes the way? *Mediators of Inflammation,* 2017(8619307): 1-11.

Mayer-Barber, K. D. and Barber, D. L. (2015). Innate and adaptive cellular immune responses to *Mycobacterium tuberculosis* infection. *Cold Spring Harbor Perspectives in Medicine,* 5(120: a018424.

McClean, C. M. and Tobin, D. M. (2016). Macrophages form, function and phenotype in mycobacterial infection: lessons from tuberculosis and other diseases. *Pathogens and Disease,* 74(7): 1-15.

Menin, Á., Fleith, R., Reck, C., Marlow, M., Fernandes, P. *et al.* (2013). Asymptomatic cattle naturally infected with *Mycobacterium bovis* present exacerbated tissue pathology and bacterial dissemination. *Plos One,* 8(1): e53884-e53884.

Menzies, F. and Neill, S. (2000). Cattle-to-cattle transmission of bovine tuberculosis. *The Veterinary Journal*, 160(2): 92-106.

Michel, A. L., Bengis, R. G., Keet, D. F., Hofmeyr, M., de Klerk, L. M. *et al.* (2006). Wildlife tuberculosis in South Africa conservation areas: Implications and challenges. *Veterinary Microbiology*, 112 (2006): 91-100.

Michel, A. L., Müller, B. and van Helden, P. D. (2009). *Mycobacterium bovis* at the animal-human interface: a problem, or not? *Veterinary Microbiology,* 140(2010); 371-381.

Michelsen, S. W., Soberg, B., Diaz, L. J., Hoff, S. T. Agger, E. M. *et al.* (2017). The dynamics of immune responses to *Mycobacterium tuberculosis* during different stages of natural infection: a longitudinal study among Greenlanders. *PLoS One,* 12(6): e0177906.

Moran, E. (2019). *Th17 cells | British Society for Immunology*. [online] Immunology.org. Available at: https://www.immunology.org/public-information/bitesized-immunology/c%C3%A9lulas/th17-cells [Accessed 27 May 2019].

Musoke, J., Hlokwe, T., Marcotty, T., du Plessis, B. J. A. and Michel, A. L. (2015). Spillover of *Mycobacterium bovis* from wildlife to livestock, South Africa. *Emerging Infectious Diseases,* 21(13): 448-451.

Mustafa, T., Mogga, S. J., Mfinanga, S. G., Mørkve, O. and Sviland, L. (2006). Immunohistochemical analysis of cytokines and apoptosis in tuberculous lymphadenitis. *Immunology,* 117(4): 454-462.

Mustafa, T., Wiker, H. G., Mørkve, O. and Sviland, L. (2008). Differential expression of mycobacterial antigen MPT64, apoptosis and inflammatory markers in multinucleated giant cells and epithelioid cells in granulomas caused by *Mycobacterium tuberculosis. Virchows Achriv,* 452(4): 449-456.

Naranjo, V., Gortazar, C., Vicente, J. and de la Fuente, J. (2008). Evidence of the role of European wild boar as a reservoir of *Mycobacterium tuberculosis* complex. *Veterinary Microbiology,* 127(1-2): 1-9.

Ncbi.nlm.nih.gov. (2020). *Resources* | *How to* | ACTB actin beta [*Homo sapiens* (human)] [online] Available at: https://www.ncbi.nlm.nih.gov/gene/60.

Nugent, G., Buddle, B. M. and Knowles, G. (2015). Epidemiology and control of *Mycobacterium bovis* infection in brushtail possums (*Trichosurus vulpecula*), the primary wildlife host of bovine tuberculosis in New Zealand. *New Zealand Veterinary Journal,* 63(1): 28-41.

Pagán, A. and Ramakrishnan, L. (2018). The formation and function of granulomas. *Annual Review of Immunology*, 36(1): 639-665.

Palmer, M. (2017). Emerging understanding of tuberculosis and the granuloma by comparative analysis in humans, cattle, zebrafish, and nonhuman primates. *Veterinary Pathology*, 55(1): 8-10.

Palmer, M., Thacker, T. C. and Waters, W. R. (2016). Multinucleated giant cell cytokine expression in pulmonary granulomas of cattle experimentally infected with *Mycobacterium bovis. Veterinary Immunology and Immunopathology,* 180: 34-39. https://doi.org/10.1016/j.vetimm.2016.08.015

Palmer, M., Thacker, T. C., Waters, W. R., Gortázar, C. and Corner, L. A. L. (2012). *Mycobacterium bovis*: a model pathogen at the interface of livestock, wildlife and humans. *Veterinary Medicine International,* 2012(236205): 1-17.

Palmer, M., Waters, W. R. and Thacker, T. C. (2007). Lesion development and immunohistochemical changes in granulomas from cattle experimentally infected with *Mycobacterium bovis*. *Veterinary Pathology*, 44(6): 863-874.

Parsons, S. D. C., Cooper, D., McCall, A. J., McCall, W. A., Streicher, E. M. *et al.* (2011). Modification of the QuantiFERON-TB Gold (In-Tube) assay for the diagnosis of *Mycobacterium bovis* infection in African buffaloes (*Syncerus caffer*). *Veterinary Immunology and Immunopathology,* 142(2011): 113-118.

Pearl, J. E., Saunders, B., Ehlers, S., Orme, I. M. and Cooper. A. M. (2001). Inflammation and lymphocyte activation during mycobacterial infection in the interferon-gamma-deficient mouse. *Cell Immunology,* 211(1): 43-50.

Phuah, J. Y., Mattila, J. T., Lin, P. L. and Flynn, J. L. (2012). Activated B cells in the granulomas of nonhuman primates infected with *Mycobacterium tuberculosis*. *American Journal of Pathology,* 181(2): 508-514.

Rajasekaran, S., Mahilmaran, A., Annadurai, S., Kumar, S. and Raja, K. (2007). Manifestation of tuberculosis in patients with human immunodeficiency virus: a large Indian study. *Annals of Thoracic Medicine,* 2(2): 58-60.

Ramakrishnan, L. (2012). Revisiting the role of the granuloma in tuberculosis. *Nature Reviews Immunology*, 12(5): 352-366.

Ramos, D. F., Silva, P. E. A. and Dellagostin, O. A. (2015). Diagnosis of bovine tuberculosis: review of main techniques. *Brazilian Journal of Biology,* 75(4): 830-837.

Renwick, A. F., White, P.C. and Bengis, R. G. (2007). Bovine tuberculosis in southern African wildlife: a multi-species pathogen system. *Epidemiology and Infection*, 135(4): 529-540.

Rodwell, T. C., Kriek, N. P., Bengis, R. G., Whyte, I. J., Viljoen, P. C. *et al.* (2001). Prevalence of bovine tuberculosis in African buffalo at Kruger National Park. *Journal of Wildlife Diseases,* 37(2): 258-264.

Rusk, R. A., Palmer, M. V., Waters, W. R. and McGill, J. L. (2018). Measuring bovine T cell function at the site of *Mycobacterium bovis* infection. *Veterinary Immunology and Immunopathology,* 193-194: 28-49. https://doi.org/10.1016/j.vetimm.2017.10.004

Salguero, F. J., Gibson, S., Garcia-Jimenez, W., Gough, J., Strickland, T. S. *et al.* (2016). Differential cell composition and cytokine expression within lymph node granulomas from BCG-vaccinated and non-vaccinated cattle experimentally infected with *Mycobacterium bovis. Transboundary and Emerging Diseases,* 64(6): 1734-1749.

Sanchez, J., Tomás, L., Ortega, N., Buendía, A., del Rio, L., Salinas, J., Bezos, J., Caro, M. and Navarro, J. (2011). Microscopical and immunological features of tuberculoid granulomata and cavitary pulmonary tuberculosis in naturally infected goats. *Journal of Comparative Pathology*, 145(2-3): 107-117.

Sasindran, S. and Torrelles, J. (2011). *Mycobacterium tuberculosis* infection and Inflammation: what is beneficial for the host and for the bacterium? *Frontiers in Microbiology*, 2(2): 1-16

Shaler, C. R., Horvath, C. N., Jeyanathan, M and Xing, Z. (2013). Within the enemy's camp: contribution of the granuloma to the dissemination, persistence and transmission of *Mycobacterium tuberculosis*. *Frontiers in Immunology*, 4(3): 1-5.

Shankar Subramanian Iyer, G. (2019). *Role of interleukin 10 transcriptional regulation in inflammation and autoimmune disease*. [online] PubMed Central (PMC). Available at: https://www.ncbi.nlm.nih.gov/pmc/articles/PMC3410706/ [Accessed 27 May 2019].

Smith, K., Bernitz, N., Goldswain, S., Cooper, D., Warren, R. M. *et al.* (2021). Optimized interferon-gamma release assays for detection of *Mycobacterium bovis* infection in African buffaloes (*Syncerus caffer*). *Veterinary Immunology and Immunopathology,* 231(2021): 1-7

Smith, K., Bernitz, N., Cooper, D., Kerr, T. J., de Waal, C. *et al.* (2021). Optimisation of the tuberculin skin test for detection of *Mycobacterium bovis* in African buffaloes (*Syncerus caffer*). *Preventive Veterinary Medicine,* 188(2021): 1-6.

Tadayon, K., Mosavari, N., Shahmoradi, A., Sadeghi, F., Azarvandi, A. and Forbes, K. (2006). The epidemiology of *Mycobacterium bovis* in buffalo in Iran. *Journal of Veterinary Medicine Series B*, 53(s1): 41-42.

TeKippe, E., Allen, I., Hulseberg, P., Sullivan, J., McCann, J., Sandor, M., Braunstein, M. and Ting, J. (2010). Granuloma formation and host defence in chronic *Mycobacterium tuberculosis* infection requires PYCARD/ASC but not NLRP3 or Caspase-1. *PLoS ONE*, 5(8), p.e12320.

Tesmer, L., Lundy, S., Sarkar, S. and Fox, D. (2008). Th17 cells in human disease. *Immunological Reviews*, 223(1): 87-113.

Ulrichs, T., Kosmiadi, G. A., Trusov, V., Jorg, S., Pradl, L. *et al.* (2004). Human tuberculous granulomas induce peripheral lymphoid follicle-like structures to orchestrate local host defence in the lung. *Journal of Pathology,* 204(2): 217-228.

Viljoen, I. M., van Helden, P. and Millar, R. P. (2015). *Mycobacterium bovis* infection in the lion (*Panthera leo*): Current knowledge, conundrums and research challenges. *Veterinary Microbiology,* 177(3-4): 252-260.

Wangoo, A., Johnson, L., Gough, J., Ackbar, R., Inglut, S., Hicks, D., Spencer, Y., Hewinson, G. and Vordermeier, M. (2005). Advanced granulomatous lesions *in Mycobacterium bovis*-infected cattle are associated with increased expression of type I procollagen, γδ (WC1+) T cells and CD 68+ Cells. *Journal of Comparative Pathology*, 133(4): 223-234.

Waters, W. R. and Palmer, M. V. (2015). *Mycobacterium bovis* infection of cattle and white-tailed deer: translational research of relevance to human tuberculosis. *ILAR Journal,* 56(1): 26-43.

Warsinske, H. C., DiFazio, R. M., Linderman, J. J., Flynn, J. L. and Kirschne, D. E. (2017). Identifying mechanisms driving formation of granuloma-associated fibrosis during *Mycobacterium tuberculosis* infection. *Journal of Theoretical Biology,* 429(8): 1-17.

World Health Organization. 2010. Treatment of tuberculosis guidelines, 4th ed World Health Organization, Geneva, Switzerland. https://www.who.int

Werner, M., Chott, A., Fabiano, A. and Battifora, H. (2000). Effect of formalin tissue fixation and processing on immunohistochemistry. *Journal of Surgical Pathology,* 24(7): 1016-1019.

Wieczorek, M., Abualrous, E. T., Sticht, J., Álvaro-Benito, M., Stolzenberg, S, *et al.* (2017). Major histocompatibility complex (MHC) class I and MHC class II proteins: conformational plasticity in antigen presentation. *Frontiers in Immunology,* 292(8): 1-16.

Yuan, L., Ke, Z., Ma, J., And Li, Y. (2015). The fluorescence in situ hybridization for diagnosis of *Mycobacterium tuberculosis* complex in sputum samples. *Annals of Clinical & Laboratory Science,* 45(6): 631-638.

Zhu, Q., Han, X., Peng, J., Qin, H., Wang, Y. *et al.* (2012). The role of CXC chemokines and their receptors in the progression and treatment of tumors. *Journal of Molecular Histology,* 43(6): 699-713.

Appendices

Appendix 1

Summary of cytokine release assays (QFT IPRA, Bovigam assay and QFT IGRA), SCITT, tissue mycobacterial culture results and gross lesion scores of tissues selected from HiP 2018 buffaloes used for histopathological analysis.

Buffalo #	Gross score	Culture result	SCITT	QFT IPRA	Bovigam	QFT IGRA
1 (458/19)	3	Pos	Pos	Pos	Pos	Neg
2 (460/19)	3	Pos	Pos	Neg	Pos	Neg
3 (463/19)	2	Pos	Pos	Pos	Neg	Invalid
4 (467/19)	1	Pos	Neg	Pos	Pos	Invalid
5 (470/19)	3	Pos	Pos	Neg	Neg	Neg
6 (472/19)	3	Pos	Neg	Pos	Pos	Neg
7 (475/19)	1	Pos	Pos	Pos	Pos	Neg
8 (481/19)	2	Pos	Pos	Pos	Neg	Neg
9 (483/19)	3	Pos	Neg	Back	Pos	Invalid
10 (485/19)	2	Pos	Pos	Pos	Pos	Neg
11 (487/19)	2	Pos	Pos	Pos	Pos	Neg
12 (490/19)	3	Pos	Pos	Back	Pos	Neg

QFT IGRA - QuantiFERON TB-Gold interferon gamma release assay; QFT IPRA - interferon gamma-induced protein 10kDa release assay; SICTT - single intradermal comparative tuberculin test; Pos – positive; Neg – negative; UM – unmeasurable; Back – background

Appendix 2

Basic histological procedure for H&E staining, Tygerberg, Stellenbosch University. Haematoxylin and Eosin (H&E) tissue slide standard staining protocol using the Leica ST5010 Autostainer XL (Leica Biosystems, Cape Town, South Africa).

Method

1. Prior to staining slides are placed in the incubator for wax to melt off the tissue.
2. Lung tissues were stained with H&E Leica Autostainer XL with the following protocol:

Step	Step	Time (min)	Repeats
1	Oven (60°C)	2	1
2	Xylene	5	2
3	Ethanol (99%)	2	2
4	Ethanol (96%)	2	1
5	Ethanol (70%)	2	1
6	Tap water	2	1
7	Haematoxylin	8	1
8	Running water	5	1
9	Eosin	4	1
10	Running water	1	1
11	Ethanol (70%)	0.5	1
12	Ethanol (96%)	0.5	2
13	Ethanol (99%)	0.5	1
14	Xylene	1	1

Appendix 3

Ziehl-Neelsen (ZN) staining protocol used for buffalo tissue sections.

Adapted from:

1. Bancroft & Stevens, 2nd Edition 1982.
2. Amer J Clin Pathol, Vol 21, 1951.
3. Fremantle Hospital, Department of Histopathology, Western Australia.

Reagents

(1) Carbol fuchsin

New Fuchsin (C142520)	1.5gm	
Absolute alcohol	10ml	
Distilled water	10ml	
Glycerol	10ml	
Triton X100	0.75ml	

(2) Stock Methylene blue

Methylene blue (C152015)	2gm	
Distilled water	100ml	
Absolute alcohol	100ml	

(3) Working Methylene blue (40%)

Stock Methylene blue	40ml	
Distilled water	60ml	(stir using magnetic stirrer)
Glacial acetic acid	0.5ml	

(4) 0.5% Acid alcohol

Distilled water	700ml
Absolute alcohol	300ml
Hydrochloric acid	5ml

(5) 5% Sulphuric acid

Distilled water	475ml
Sulphuric acid	25ml

Method

1. Heat slides in dryer to facilitate dewaxing.
2. Place slides under running water for 2 minutes.

3. Drain slides and place in a slide mailer with 15ml of soft Carbol Fuchsin.
4. Fill slide mailer so that fluid comes up to slide frosting.
5. Place mailer into a microwave for 30 seconds at full power, in a beaker, in case of spillage, leave cap of mailer open.
6. Allow to stand for 2-5 minutes.
7. Wash excess stain from slide with distilled water.
8. Wash well in running water for 5 minutes, wipe away excess stain.
9. Differentiate individually with 0.5% acid alcohol for 1-3 minutes, control microscopically.
10. Wash in running water for 5 minutes.
11. Pour on Working Methylene blue for 20 seconds.
12. Wash with water.
13. Drain and air. Dry thoroughly.
14. Dip slides in DPX.

Results

Acid-fast bacilli	Red rods
Nocardia	Red, long, thin and filamentous
Erythrocytes	Pale pink

Appendix 4

Photomicrographs of H&E stained buffalo lung tissue sections used for analyses in this project, scanned at a magnification of 40x. Resolution of each image is included in the slide.

Buffalo 2 (460/19)

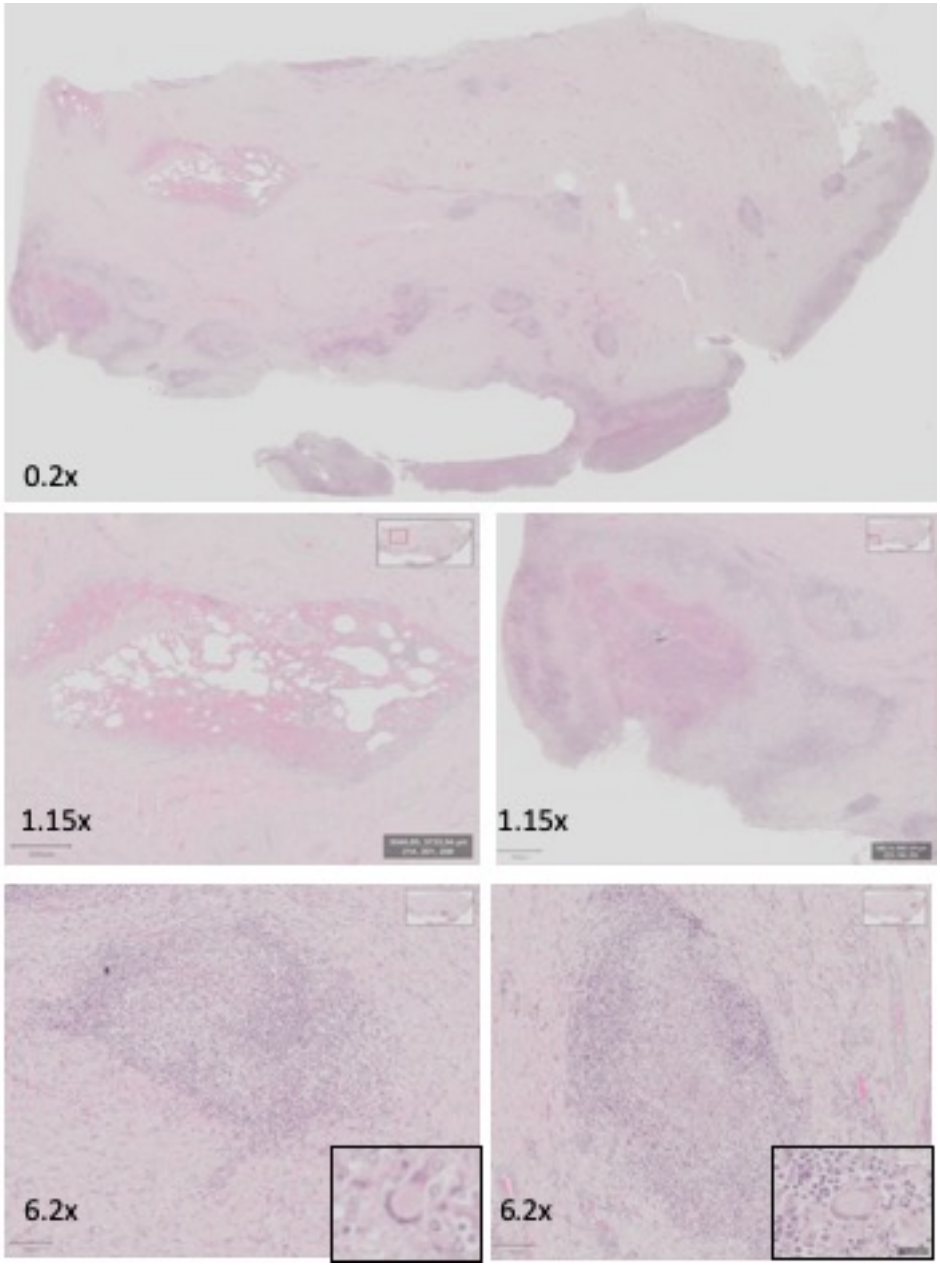

Buffalo 4 (467/19)

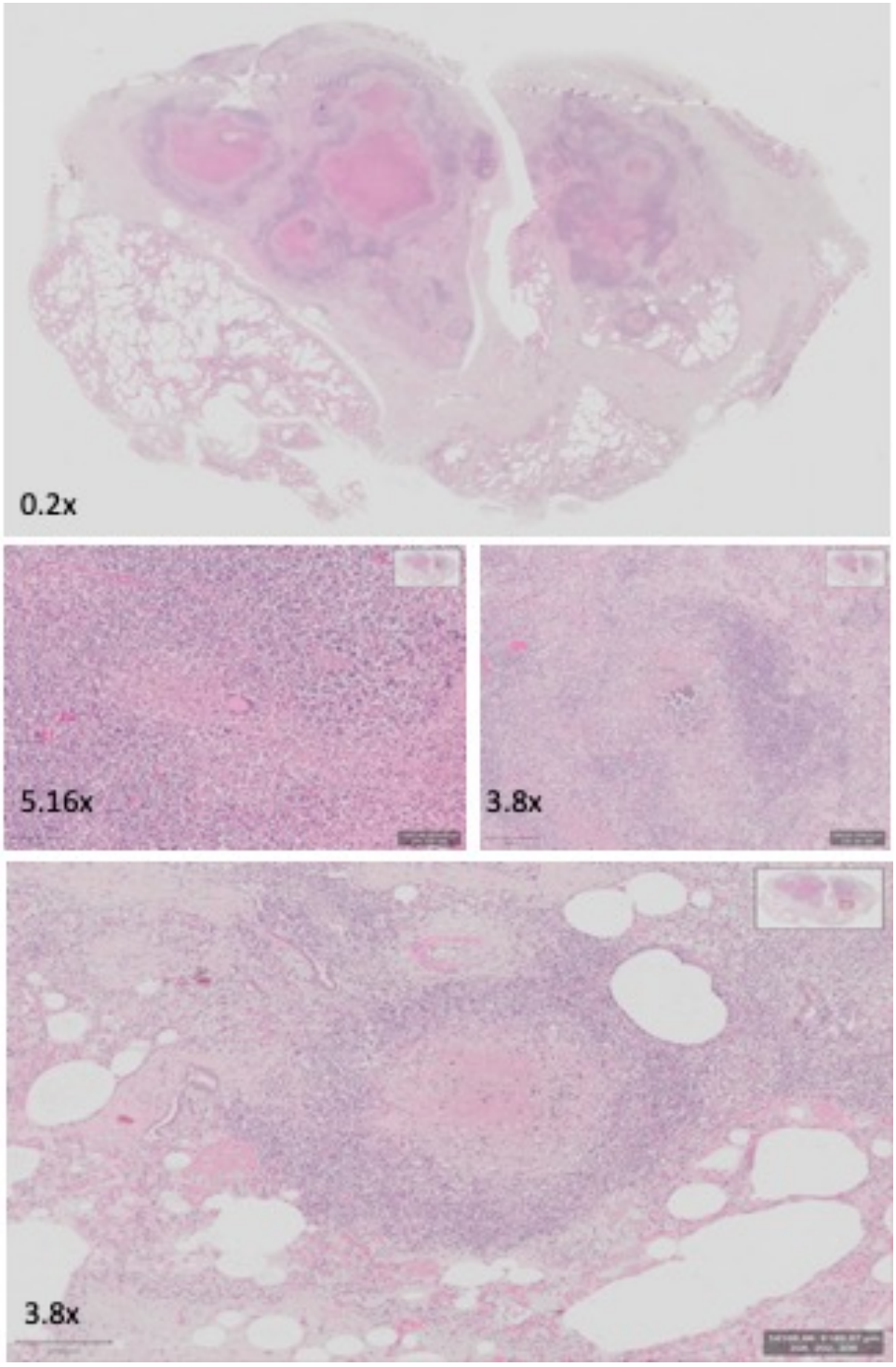

Buffalo 7 (472/19)

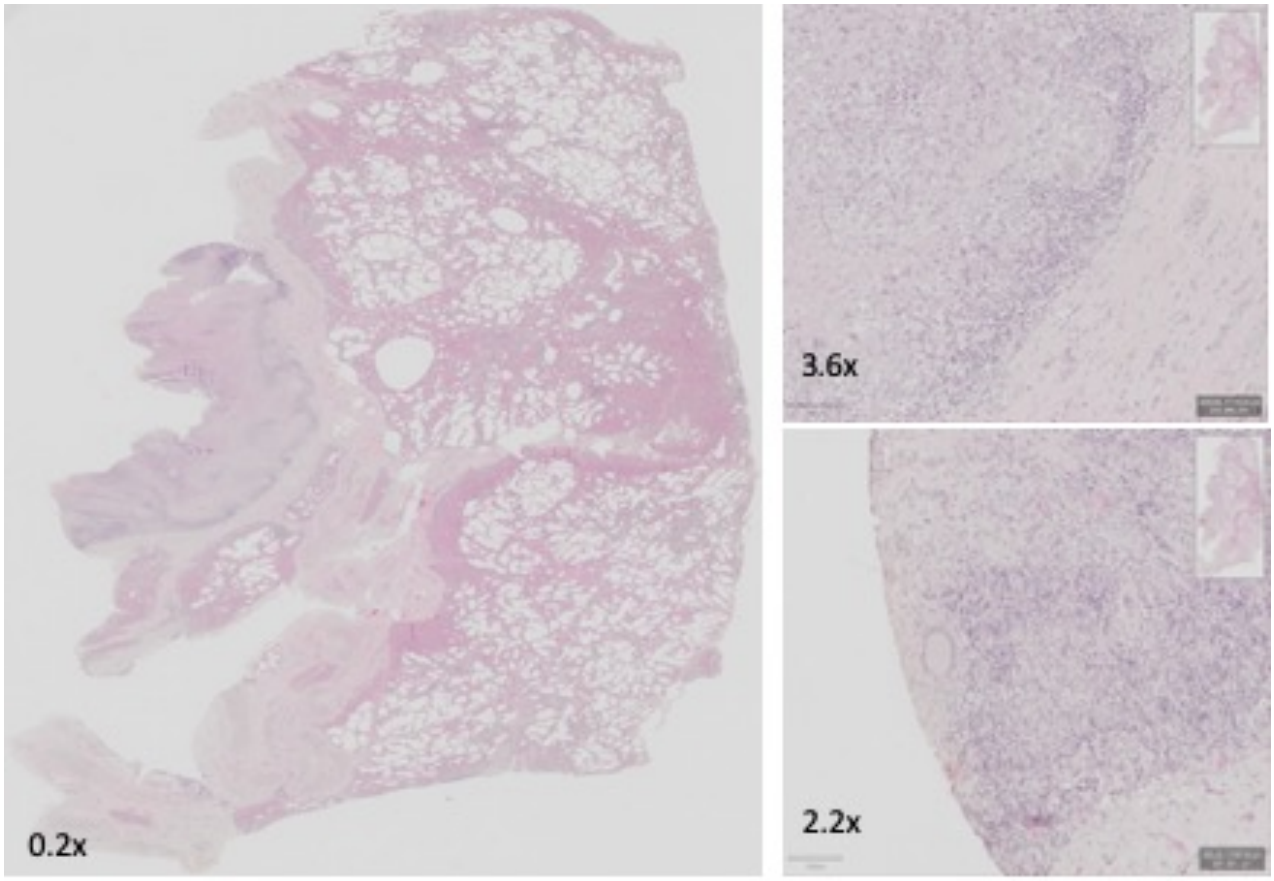

Buffalo 8 (475/19)

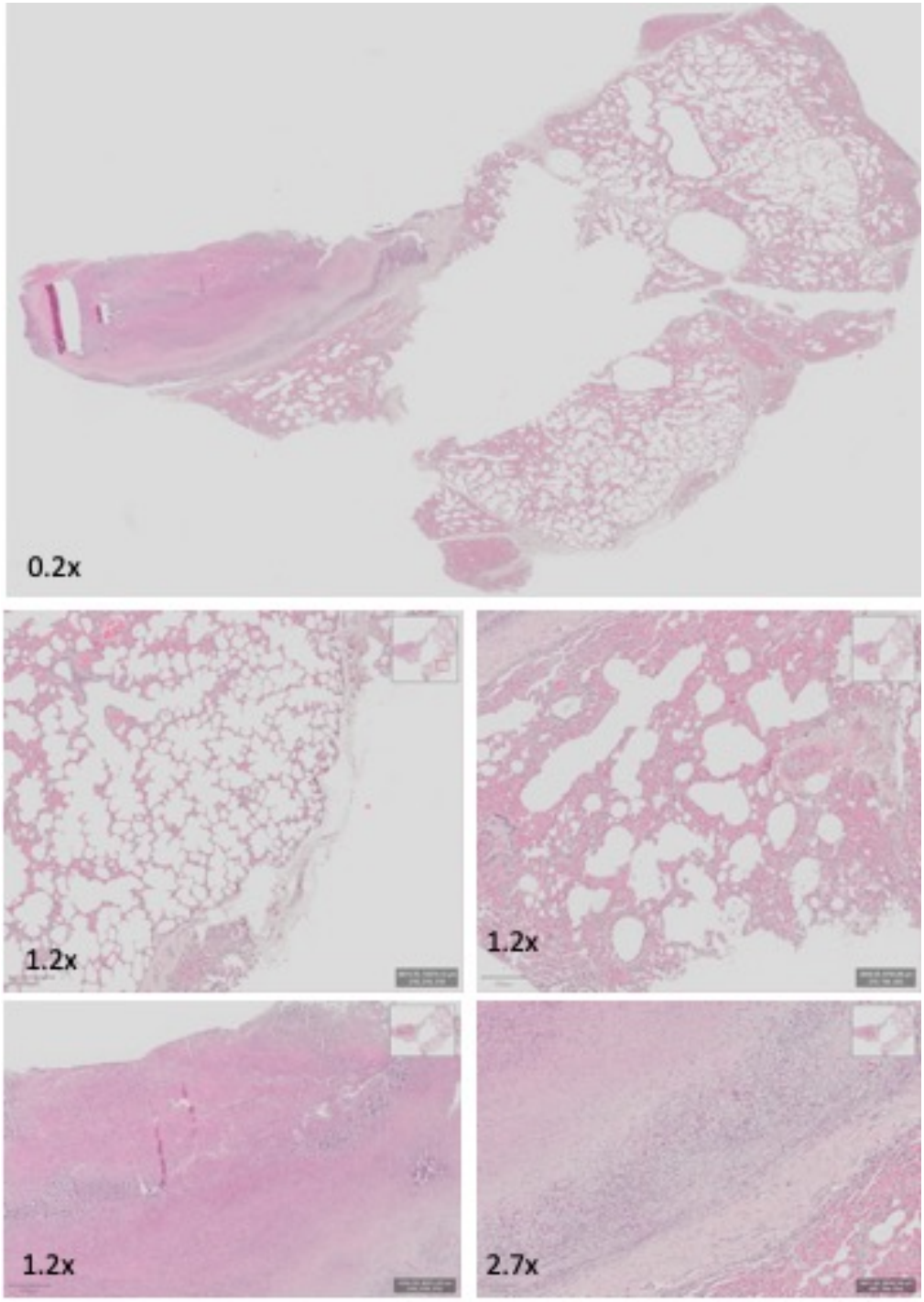

Buffalo 10 (481/19)

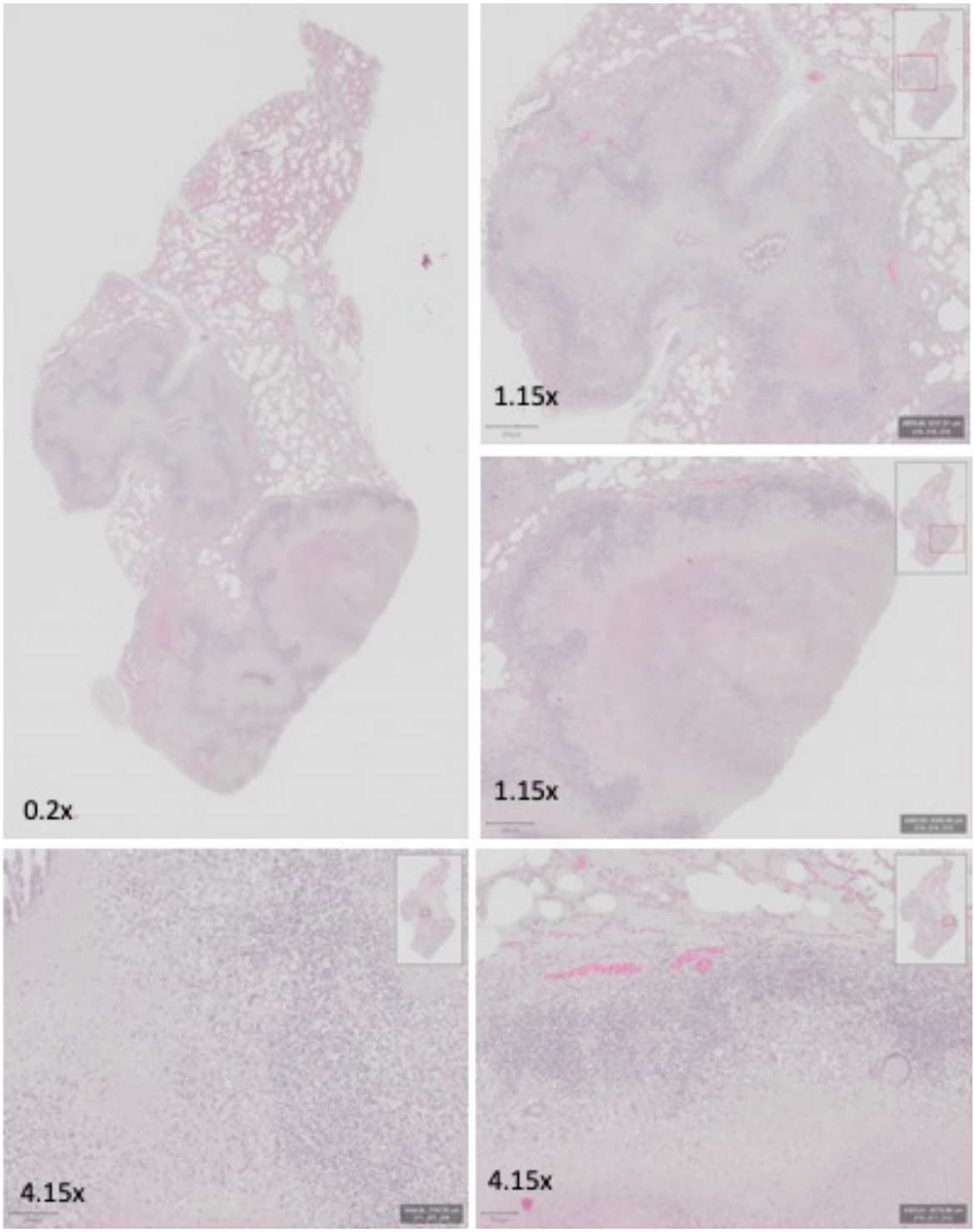

Buffalo 11 (483/19)

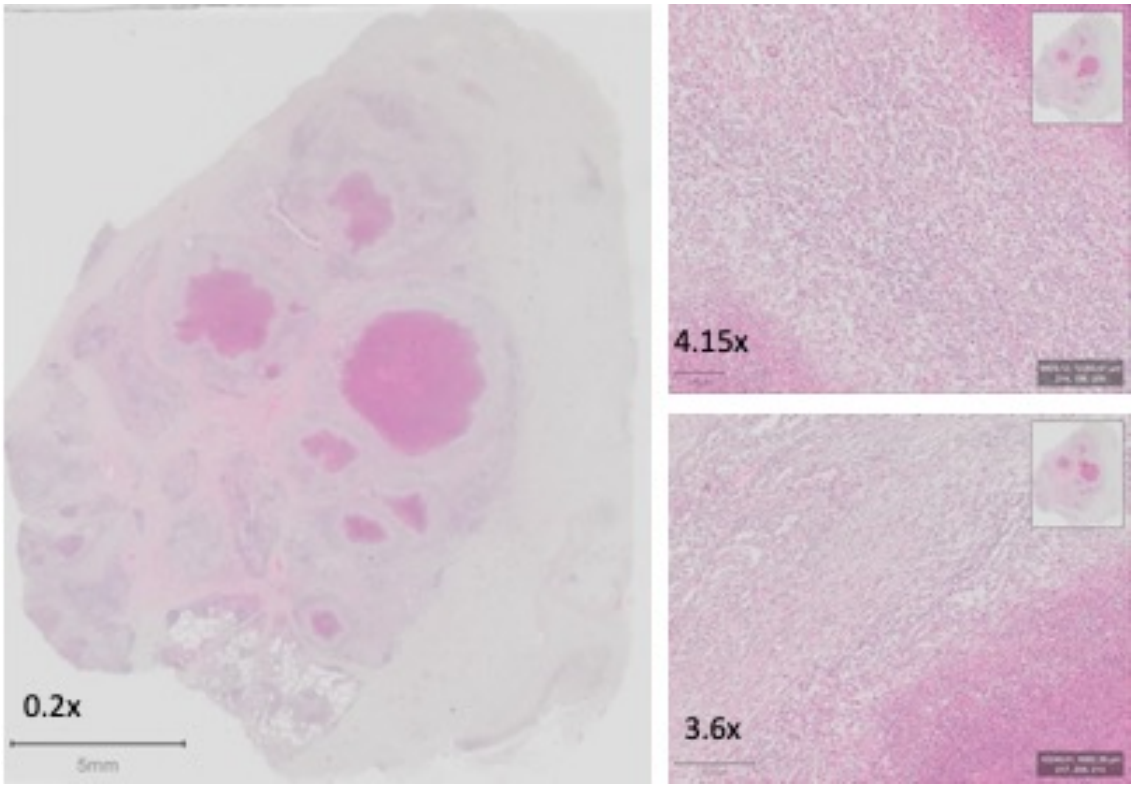

Buffalo 12 (485/19)

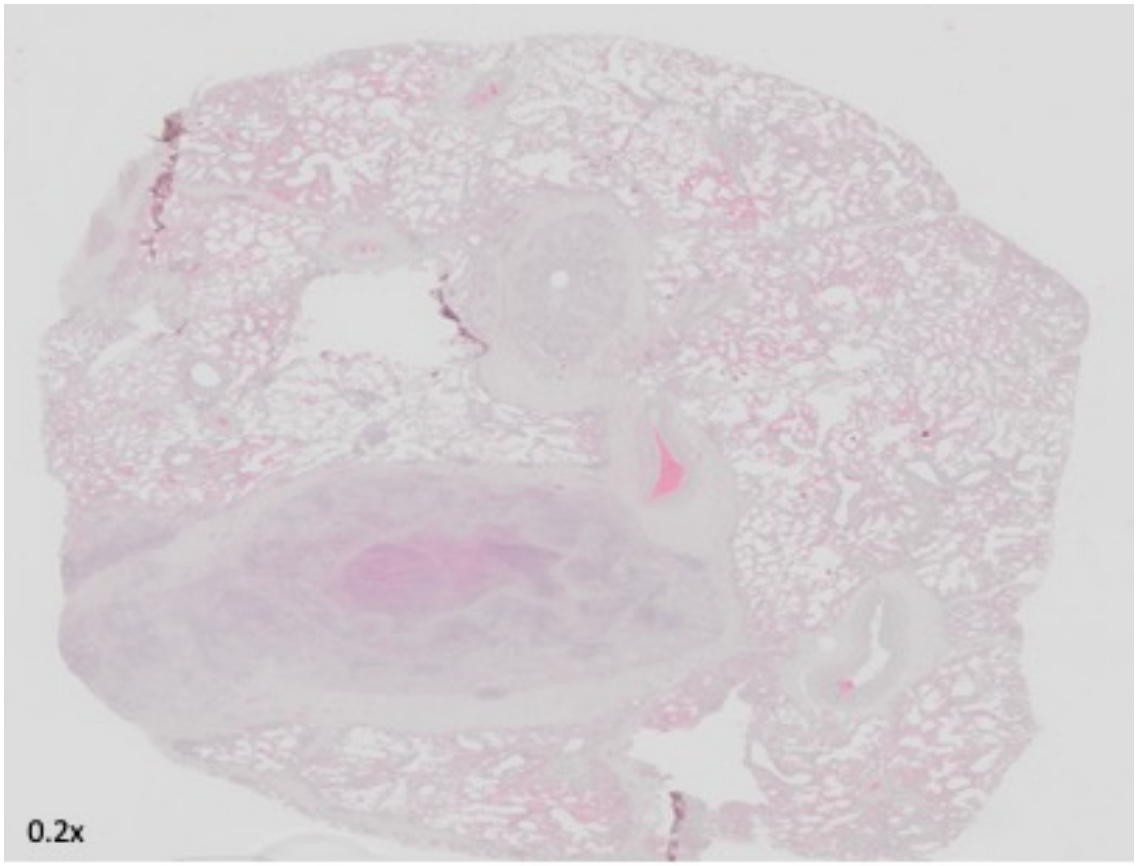

Buffalo 13 (487/19)

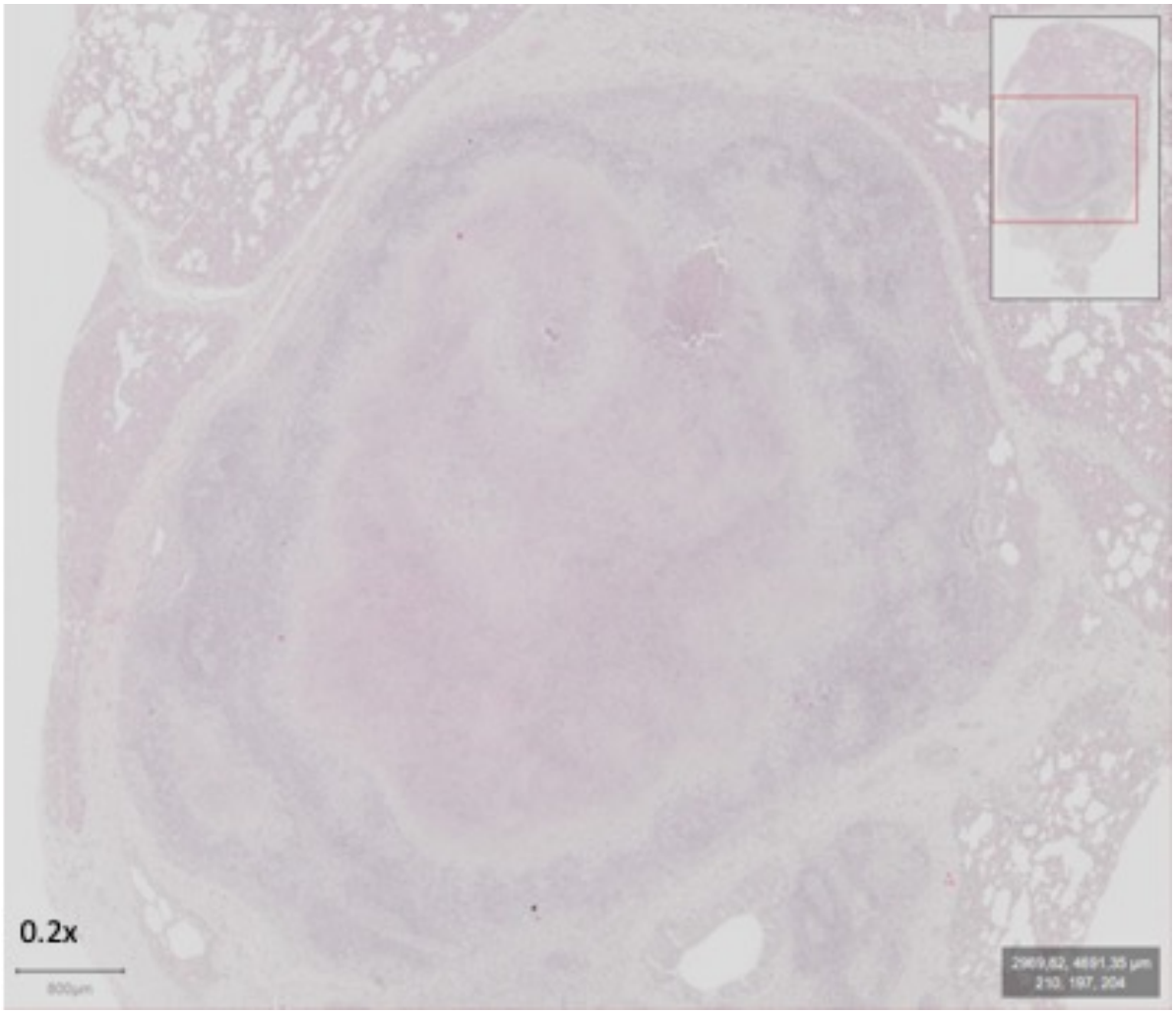

Buffalo 14 (490/19)